

## **B6: Kikai caldera and southern Kyushu: products of a large silicic magmatic system**

Fukashi MAENO\*, Keiko SUZUKI-KAMATA\*\* and Shoichi KIYOKAWA\*\*\*

\*: *Earthquake Research Institute, University of Tokyo, Japan*

\*\* : *Department of Earth & Planetary Sciences, Kobe University, Japan*

\*\*\*: *Department of Earth & Planetary Sciences, Kyushu University, Japan*

### **1. Introduction**

Kikai caldera is one of the most active volcanoes in Japan. Most of the caldera is now submerged, except two major islands, Satsuma Iwojima and Takeshima. The last caldera-forming eruption, called “Akahoya eruption”, occurred 7,300 years ago. This eruption produced voluminous pyroclastic flows (Koya ignimbrite) and widespread ash fall (Akahoya ash) that devastatingly impacted the culture and nature the western Japan. After this eruption, new volcanoes grew up inside the caldera with bimodal magmatism. One of young silicic cones, Iwo-dake, has continued to emit volcanic gases for more than hundred years.

This paper studies Satsuma Iwojima Island and southern Kagoshima area to observe the eruptive products from the Kikai caldera, and mainly focuses on pyroclastic deposits (plinian fallouts and ignimbrites with various lithofacies) from the Akahoya eruption, young tephra and lava flows from postcaldera volcanoes, and characteristic hydrothermal activities. Two young volcanoes (silicic Iwo-dake and basaltic Inamura-dake) in Satsuma Iwojima Island have spectacular scenery. The recent activities, deposits, and scenery mark the evolution of a large silicic magmatic system beneath the sea. We also study silicic pyroclastic deposits from the Ikeda caldera in Ibusuki area and those from Ata caldera in Osumi area. These eruptions also represent large-scale silicic eruptions in southern Kyushu during the late Quaternary period.

This paper is organized as follows. In Sec. 2, the tectonic setting of southern Kyushu is briefly introduced. In Sec. 3, the outline of the Kikai caldera is explained. In Sec. 4, the 7.3-ka Kikai-Akahoya eruption is highlighted. In Sec. 5, Ata caldera and Ibusuki volcanic area are focused. In Sec. 6, descriptions of Stop are summarized.

### **2. Tectonic setting of southern Kyushu**

In Kyushu, a number of large calderas have formed in the past one million years. The two major

areas of caldera formation appear to coincide with areas of extensional normal faulting, namely, the Kagoshima volcano-tectonic graben (KVTG, Fig. 1) (for Kakuto-Kobayashi, Aira, Ata and Kikai calderas) and the Beppu-Shimabara graben (for Aso caldera). The KVTG is a trough-shaped depression approximately 30 km wide and 120 km long and trending NNE-SSW across the southernmost of Kyushu Island. Quaternary volcanism in this area is confined to the wideness of the KVTG, which represents the volcanic front consisting of the northern part of the Ryukyu Arc. The graben has been subject to continuous extension and downfaulting since the late Pliocene (Shiono *et al.*, 1980; Aramaki, 1984). It can be explained by tectonics that a large part of southern Kyushu has rotated counterclockwise with respect to northern Kyushu and Eurasia Plate during the past two million years (Kodama *et al.*, 1995). There are six major calderas (Kakuto, Kobayashi, Aira, North Ata, South Ata and Kikai), all of which include postcaldera cones and lava flows, which have formed inside the graben during the late Quaternary period.

### **3. Outline of the Kikai caldera**

#### **3-1 Eruptive history before the 7.3-ka caldera-forming eruption**

Kikai caldera, 17-km wide and 20-km long, is located in the East China Sea and on the southern extension of the Kagoshima volcano-tectonic graben (KVTG). Most of the Kikai caldera is presently submerged (Fig. 2). Subaerial parts form the two main islands on the northern caldera rim, Satsuma Iwojima and Takeshima islands. Rhyolitic Iwo-dake and basaltic Inamura-dake volcanoes on Satsuma Iwojima are postcaldera stratocones (Fig. 3). The caldera floor is 300 to 500 m below the sea level and some submarine cones grew up after the caldera formation (Fig. 2). The central part of the caldera is thought to be a resurgent dome that grew up after the 7.3-ka caldera-forming eruption.



Fig. 1. Distribution of large calderas in southern Kyushu, the location of Kikai and Ata calderas, Ibusuki volcanic area and the Kagoshima volcano-tectonic graben is indicated.

Volcanic activity of the Kikai caldera began approximately 700 ka (Ono *et al.*, 1982). In the period before the caldera-forming stage, the activity was characterized by bimodal volcanism, the products of which are divided into two groups – Yahazu-yama on Satsuma Iwojima and Magome-yama and Takahira-yama on Takeshima are basaltic volcanoes, whereas the Sannoehana lava and Akasaki lava are felsic (Table 1). After this activity, multiple caldera-forming events have occurred in the last few hundred thousand years. Deposits from these eruptions are distributed on

islands around the Kikai caldera (Fig. 4). On the caldera rim, three sheets of ignimbrite are exposed. The Koabi ignimbrite, ~140 ka (K-ab; Ono *et al.*, 1982; Machida *et al.*, 2001), is on the eastern base of Takeshima and the northern base of Satsuma Iwojima. The Nagase ignimbrite (K-Ns; Ono *et al.*, 1982) erupted at ~95 ka and is only found on Takeshima. The last ignimbrite was derived from the 7.3-ka Koya-Takeshima pyroclastic flow (K-Ky; Ui, 1973; Ono *et al.*, 1982). On both Satsuma Iwojima and Takeshima, the Komorikō tephra group (K-Km), which represents tephra layers more than 10-m thick,

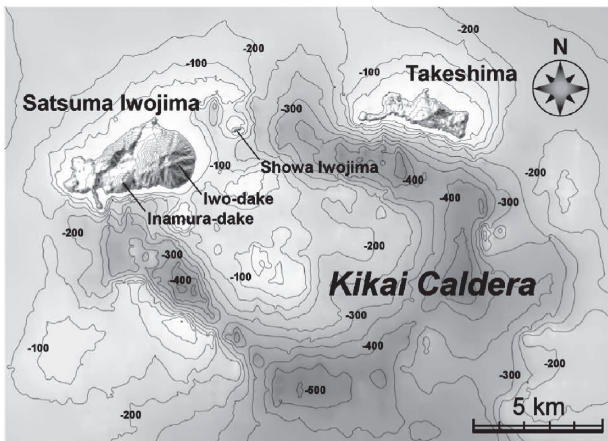


Fig. 2. Geomorphological map of the Kikai caldera. Inside the caldera the postcaldera volcanoes, Iwo-dake, Inamura-dake, and Showa Iwojima volcanoes grew up.



Fig. 3. View of Satsuma Iwo-jima from the west. A cone forward is basaltic Inamura-dake and another cone backward is rhyolitic Iwo-dake.

was deposited and the  $^{14}\text{C}$  age indicates that this activity occurred from 13 to 8 ka (Okuno *et al.*, 2000). The Nagahama lava, which comprises the western side of Satsuma Iwojima, erupted immediately before the 7.3-ka Koya eruption (Kobayashi and Hayakawa, 1984), but the precise age is unknown.

### 3-2 Eruptive history after the 7.3-ka caldera-forming eruption

Postcaldera volcanic activity started from 5.2 ka (Okuno *et al.*, 2000) with the growth of the old Iwo-dake volcano on the northwestern side of the caldera. Activities of the Inamura-dake volcano started from 3.6 ka (Okuno *et al.*, 2000). Inside the

Table 1 Geological units in Kikai caldera area

Eruptive stage	Maeno and Taniguchi (2005)			Kawanabe and Saito (2002)		Other studies	
	Tephra	Lava	Volcaniclastic rock	Name	Age (yBP)	Name	Age (yBP for no unit)
<i>Showa Iwojima Eruption</i>							1934-35 A.D.
	Stage Ylo-IV	Ylo4a-b		K-Sk-u-4	920±40	K-Iw-P2	610±30
	Stage Ylo-III	Ylo3a-c		K-Sk-u-3	940±40	K-Iw-S1 K-Iw-P1	1130±40
<i>Young Iwo-dake</i>	Stage Ylo-II	Ylo2a-e	loLF loLD, E loLB, C loLA	lo Ta (loSP)	K-Sk-u-2		
	Stage Ylo-I	Ylo1	loHy-1, u		K-Sk-u-1		2210±40
	Stage In-IV	In1L					2250±60 (2) 3040±120 (1)
<i>Inamura-dake</i>	Stage In-III	In3				K-In-2	
	Stage In-II	In2	InEL				
	Stage In-I	In1	InSL			K-In-1	3890±40
<i>Old Iwo-dake</i>	Stage Olo-II	Olo2a-b				K-Sk-l-2	
	Stage Olo-I	Olo1a-b				K-Sk-l-1	5200±70 (2)
<i>Caldera-forming stage</i>	<i>Caldera-forming eruption (Kikai-Akahoya Eruption)</i>		Koya-Takeshima pfl (K-Tk, K-Ky, K-Ah)		7.3 ka (3)		
			Funakura pfl				
			Funakura pfa (K-Kyp)				
			Nagahama lava (rhyolite)				
		Komoriko tephra group (K-Km)		13-8 ka (2)			
		<i>Caldera forming eruption</i>		Nagase pfl (K-Ns, K-Tz)		95 ka (4)	
		<i>Caldera forming eruption</i>		Koabi pfl (K-ab)		140 ka (4)	
<i>Pre-caldera-forming stage</i>	<i>Felsic lava goup</i>		Sannoehana lava, Akasaki lava				
	<i>Mafic lava goup</i>		Yahaziyama, Magomeyama, Takahirayama		700 ka- (1)		

(1) Ono *et al.* (1982), (2) Okuno *et al.* (2000), (3) Machida and Arai (2003), (4) Machida *et al.* (2001)

pfl: pyroclastic flow, pfa: pumice fall.

caldera wall on Satsuma Iwojima, rhyolitic and basaltic lavas and tephras have been formed by the Iwo-dake and Inamura-dake volcanoes (Ono *et al.*, 1982; Kawanabe and Saito, 2002; Maeno and Taniguchi, 2005). The volcanic activity is divided into three main stages and ten substages based on interpretation on the evolution of volcanic edifice and tephra deposits (Table 1): the old Iwo-dake stage (Stage OIo-I~II), the Inamura-dake stage (Stage In-I~IV), and the young Iwo-dake stage (Stage YIo-I~IV; Maeno and Taniguchi, 2005). A noticeable feature of this bimodal activity is that the basaltic activity of Inamura-dake was sandwiched between the rhyolitic activities of old and young Iwo-dake volcanoes. The rhyolitic products contain plagioclase phenocrysts as the most abundant mineral, and clinopyroxene, orthopyroxene, and magnetite and ilmenite, while the basaltic products contain plagioclase phenocrysts as the most

abundant mineral, and clinopyroxene, orthopyroxene, olivine, and magnetite and ilmenite.

The old Iwo-dake stage started with phreatomagmatic eruptions and pumice fallouts (Stage OIo-I), followed by the effusion of rhyolitic lava with continuous ejection of ash and lithic fragments, resulting in the building of the old volcanic edifice (Stage OIo-II). In the Stage OIo-II, intermittent explosive eruptions also occurred. Whole-rock composition of the Old Iwo-dake stage approximately lays on the trend of the products from the 7.3 ka caldera-forming eruption (Fig. 5). The Inamura-dake stage is characterized by basaltic lava flows and tephras, producing a small stratocone (Stage In-I~II, Fig. 5). After that, at the western foot of the cone, phreatomagmatic explosions occurred (Stage In-III), accompanied with effusive eruption of andesitic lava (Stage In-IV). In the young Iwo-dake stage, the explosive eruption occurred at

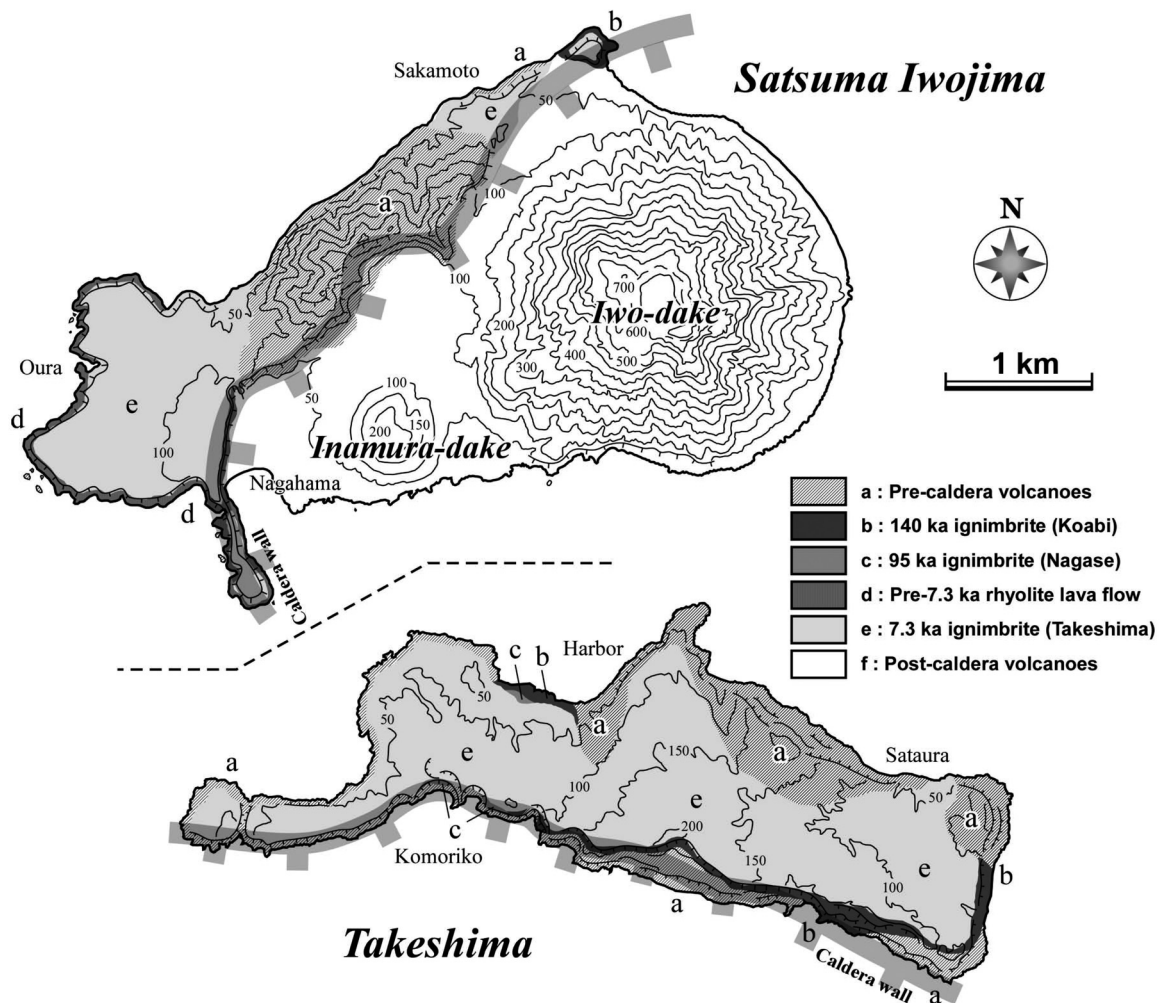


Fig. 4. Geological map of Satsuma Iwojima and Takeshima. Outside the caldera wall of the two islands, there are at least three major ignimbrite sheets (modified from Ono *et al.*, 1982).

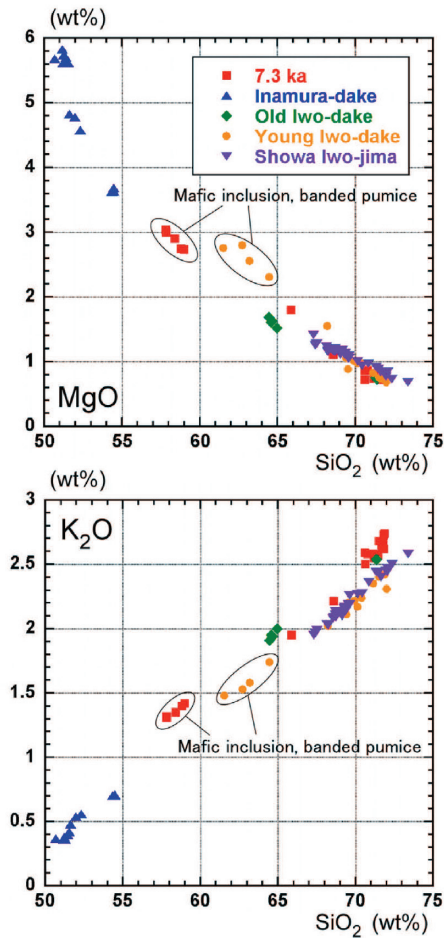


Fig. 5. Whole-rock SiO<sub>2</sub> variation diagram for MgO (upper) and K<sub>2</sub>O (bottom) for eruptive products of the Kikai caldera after the 7.3 ka caldera-forming eruption.

the beginning (Stage YIo-I), followed by the effusion of multiple rhyolitic lava flows from the summit crater and the formation of hyaloclastite in

shallow sea that made up a marine terrace (Stage YIo-II). Whole rock composition of the young Iwo-dake stage made the similar trend to the silicic products before the Inamura-dake stage, but is relatively poor in K<sub>2</sub>O (Fig. 5).

During the past 1000 years, the volcanic activity of Iwo-dake has been intermittent, with some pumice and bomb fallouts (Stage YIo-III~IV). The total phenocryst content of the Iwo-dake lavas has increased by 8% from 9 to 17 vol.% during the young stage (Fig. 6).

In 1934-35, a new silicic lava dome, Showa Iwojima Island, was formed by a submarine eruption between Satsuma Iwojima and Takeshima, which is the latest magmatic eruption in the Kikai caldera (Tanakadate, 1935; Maeno and Taniguchi, 2006). Whole-rock composition of erupted magma was gradually changed from dacitic (~67 wt% in SiO<sub>2</sub>) in early to rhyolitic (~73 wt% in SiO<sub>2</sub>) in later stage, as evidenced by the compositional zoning of lava dome (Fig. 7).

Geochemical and petrographical studies of the silicic products, the mafic inclusions, and the banded pumices from the volcanoes indicate that a stratified magma chamber exists beneath the caldera, consisting of a lower basaltic layer, an upper rhyolitic layer, and a thin middle layer of andesite during the postcaldera stage (Saito *et al.*, 2002).

Most of postcaldera activities seem to have occurred in trending with the northwestern side of the caldera. The distribution of the 7.3-ka deposits and postcaldera volcanoes indicates that the source of both rhyolite and basalt has coexisted beneath the northwestern side of the caldera during past > 7000 years (Saito *et al.*, 2002; Maeno and Taniguchi,

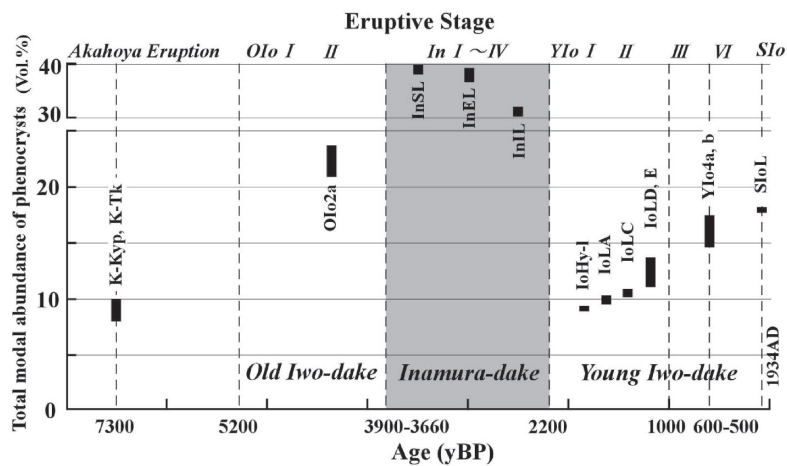


Fig. 6. Variations of modal abundance of phenocryst in volcanic rocks over the past 7300 years. Stage OIo-II is more crystal-rich (> 20 vol.%) than other stages (< 20 vol.%). In the Young Iwo-dake stage, the modal abundance increases gradually with decreasing age (modified from Maeno and Taniguchi, 2005).

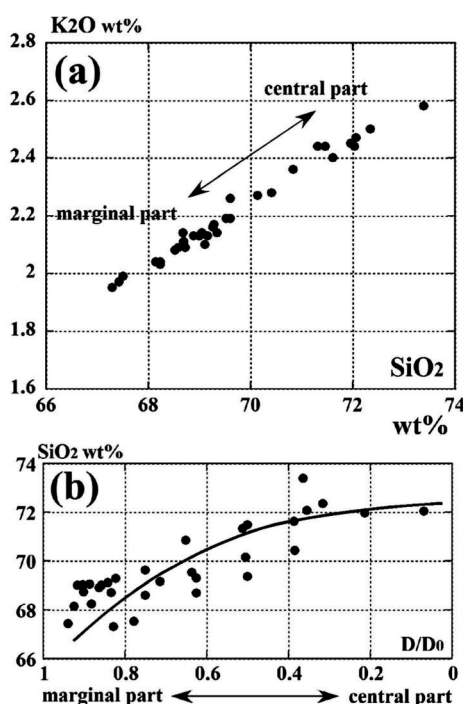


Fig. 7. (a) SiO<sub>2</sub>-K<sub>2</sub>O diagram for Showa Iwojima dome samples. (b) Compositional variation of the lava dome for normalized distance (D/D<sub>0</sub>) from the vents. The samples from the marginal part are SiO<sub>2</sub>-poor, whereas those from the dome center are SiO<sub>2</sub>-rich. Modified from Maeno and Taniguchi (2006).

2007). It is also noticeable that the location of vents is consistent with the southern extension of the western boundary of the KVTG (Fig. 1). These lines of evidence indicate that the Kikai caldera is still very active and tends to bimodal activity in the northwestern side, probably associated with the structural weakness of the caldera margin, or extensional faults in the southwestern edge of the KVTG (Maeno and Taniguchi, 2007).

### 3-3 Recent activities of the Iwo-dake volcano

Although there is a long history of sulfur mining at the summit of Iwo-dake, where the degassing activity has lasted more than several hundreds of years, no summit eruptions have been recorded in historical time. Large changes in the surface manifestation of degassing activity were observed from 1990 to 1999 at the summit crater (Shinohara *et al.*, 2002). During this period, a new degassing vent formed in the center of the crater floor. Continuous-to-intermittent volcanic ash emissions have occurred, but they appear not to have affected the relatively constant degassing activity in terms of temperature, gas composition, and emission rates. The ash emissions occurred without any explosions, even at the beginning of the intermittent ash

emissions, implying that significant pressure accumulation did not occur before ash emission activity (Shinohara *et al.*, 2002). Because the column height was quite low, commonly only a few hundred meters, the ash deposits are restricted to the area immediately around the summit crater. The volcanic ash consists of a fine material of highly altered volcanic rocks, which are likely to alter older deposits formed in the summit crater. The ash emissions are likely caused by partial collapse of the crater floor at depth and ejection of the collapsed materials by strong flow of volcanic gases (Shinohara *et al.*, 2002). The continuous and intense degassing at Satsuma Iwojima is likely caused by volatile transport from a deep magma chamber through a convecting magma column (Kazahaya *et al.*, 2002).

### 3-4 Volcanic gas and Hot springs in Satsuma Iwojima

Satsuma Iwojima is characterized by intense emission of high-temperature volcanic gases. There has been degassing activity in the last 30 years and possibly for more than several hundreds of years (Shinohara *et al.*, 2002). At the beginning of quantitative observation of the volcano (in the 1990s), the maximum measured temperature of the fumaroles was constant ranging from 840 to 900°C, which is close to the temperature of the rhyolitic magma beneath the caldera (~970°C; Saito *et al.*, 2001). Measured volcanic SO<sub>2</sub> gas emission rates were also constant between 500-1000 t/d (Kazahaya *et al.*, 2002). The high-temperature fumaroles are distributed only in and around the summit crater, while low-temperature fumaroles are distributed not only at the summit but also on the volcano flanks, mainly along valleys. Because the temperature of volcanic gases is so high, the high-temperature fumarolic areas are highly altered to grayish ash with various high temperature sublimates. Volcanic rocks at the summit are highly silicified due to acid leaching. The leachates are discharged as acid sulfate hot springs distributed along the coast at the foot of the volcano.

### 3-5 Hydrothermal evidence and iron sedimentation at Nagahama Bay

The Satsuma Iwojima Island is characterized by a shallow-water hydrothermal activity where orange-brown and brown-white discharges can be found along the shoreline. Such coloring occurs due to precipitation of Fe- and Al-bearing minerals as a result of the neutralization and the oxidation of acidic hydrothermal fluids that contain high concentrations of Fe and Al (Kamada, 1964;



Fig. 8. Overview of Nagahama Bay. Sites of turbidity measurements in 2007 are labeled P1–P10; those in 2008 are labeled S1–S10.

Nogami *et al.*, 1993; Shinohara *et al.*, 1993; Hedenquist *et al.*, 1994). The iron-rich hydrothermal discharge of clear hot spring water around the island is quickly colored after mixing with seawater, which induces ferric iron precipitation. The acid sulfate hot springs, such as Higashi hot spring, are characterized by whitish to greenish discolored water that is due to hydrated oxides formed when the aluminum- and iron-rich acidic waters mix with seawater. The colored water diffuses into a rocky and pebbly coastline of the island, which is subject to strong wave action and ocean currents. These hydrological factors make it difficult to study depositional mechanisms for iron hydrate (or

oxides) along the coastline.

Nagahama Bay is an excellent place for studying sedimentation of iron-oxyhydroxides by shallow-marine low-temperature hydrothermal activity (Fig. 8). Its fishing port has a narrow entrance that limits exchange of seawater between the bay and the open ocean, allowing the accumulation of fine-grained precipitates of iron-bearing materials (Fe-oxyhydroxides) on the seafloor. The fishing port is usually filled with orange- to brown-colored Fe-rich water, and deposits > 1.5 m thick Fe-rich sediments. To better understand sedimentary mechanisms of Fe-rich



Fig. 9. Overview of topographic map around Satsuma Iwojima and Showa Iwojima area. After Japan Coast Guard (2008), and Mishima-mura-Kyushu University-Windy Network mapping project in 2011.

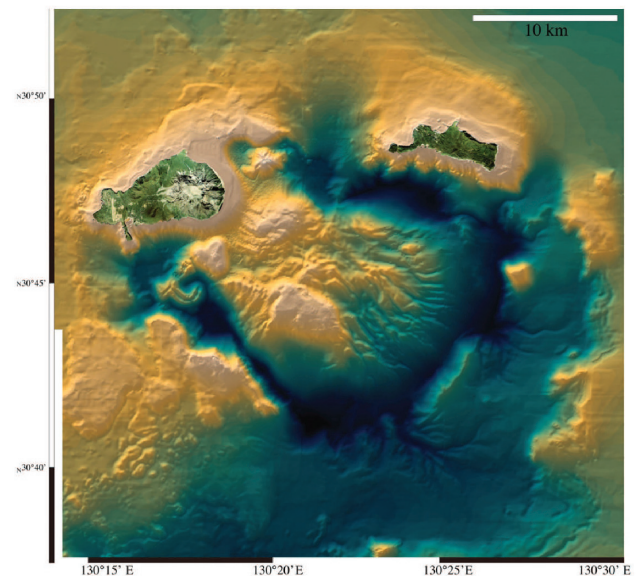


Fig. 10. Overview of the Kikai caldera. After Japan Coast Guard (2008), and Mishima-mura-Kyushu University-Windy Network mapping project in 2011.

layers under shallow-marine hydrothermal environments, an observational study has been carried out in Nagahama Bay by Kyushu University (Fig. 8), and a detailed topographic map of the bay and the wider area around the Satsuma Iwojima was obtained by Mishima village, Kyushu University, and Windy Network in 2011 (Figs. 9, 10).

Kyushu University conducted continuous profiling of turbidity throughout the tidal cycle and the monitoring of surface water. The results showed that four evidences are important, namely, wind, tide, wave, and rain. The clear seawater entered the bay during the strong north wind and rising tide, and turbid colored water flowed into the ocean during the ebb tide. Neap tide was found to be an optimal condition for sedimentation of Fe-oxyhydroxides due to weak tidal currents. Storms and heavy rains were also found to have influenced precipitation of Fe-oxyhydroxides. Storm waves disturbed the bottom sediments, resulting in increased turbidity

and rapid re-deposition of Fe-oxyhydroxides with an upward-fining sequence. Heavy rain carried Fe-oxyhydroxides originally accumulated in nearby beach sands to the bay. Their findings provide information on optimal conditions for the accumulation of Fe-rich sediments in shallow-marine hydrothermal settings.

#### 4. The 7.3-ka Kikai-Akahoya eruption

The 7.3-ka Kikai caldera eruption is the most recent and notable caldera-forming eruption in Japan during the Holocene period (Machida and Arai, 1978; 2003). The eruption occurred in a shallow sea, and produced ignimbrite and co-ignimbrite ash fall, which devastated prehistoric human settlements in southern Kyushu. The volcanic explosivity index (VEI) was 7, based on total volume of products (150-170 km<sup>3</sup>), which is a larger scale than the celebrated Santorini and Krakatau eruptions (VEI 6), and has the largest VEI

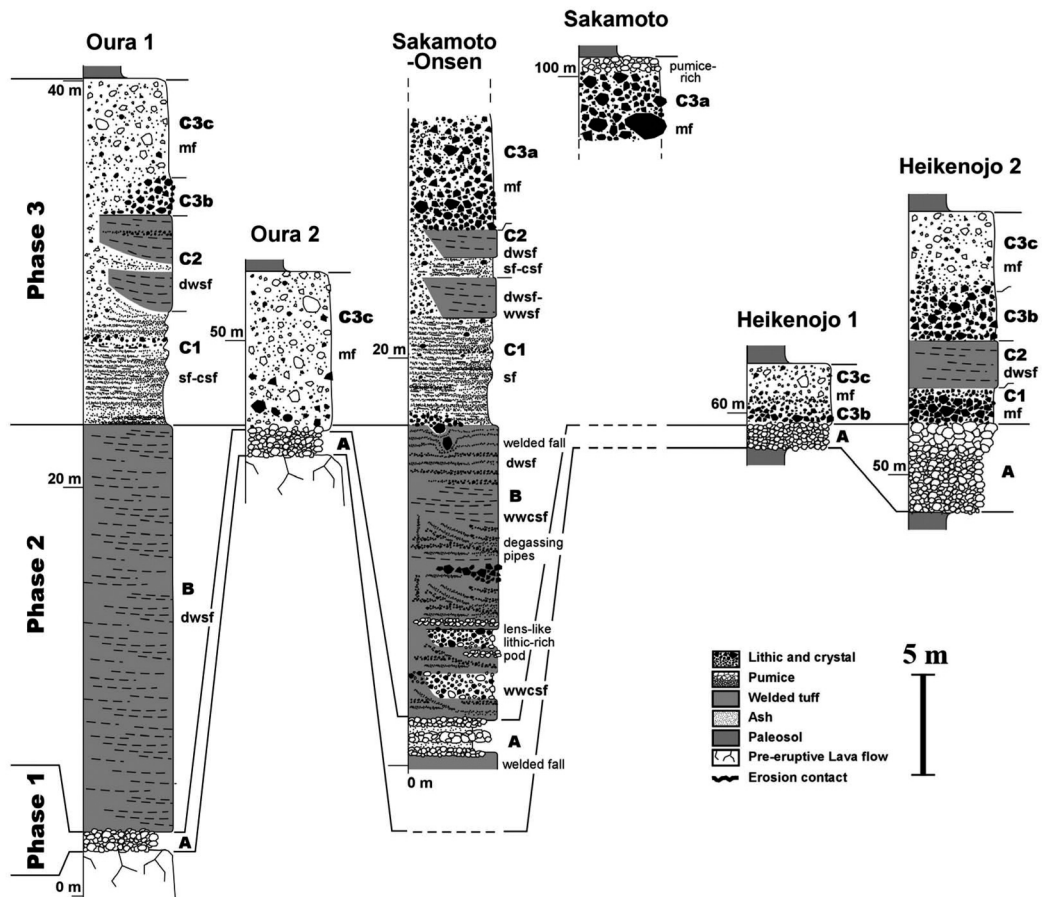


Fig. 11. Representative stratigraphic columns through the 7.3-ka eruptive deposits in Satsuma Iwojima. Deposits are divided into three main units (Units A-C). mf: non-welded massive facies, dwmf: densely welded massive facies, sf: non-welded stratified facies, wwsf: weakly welded stratified facies, dwsf: densely welded stratified facies, csf: cross-stratified facies, wwcsf: weakly welded cross-stratified facies, dwcsf: densely welded cross-stratified facies. Units A and C are subdivided into four and three subunits, respectively (modified from Maeno and Taniguchi, 2007).

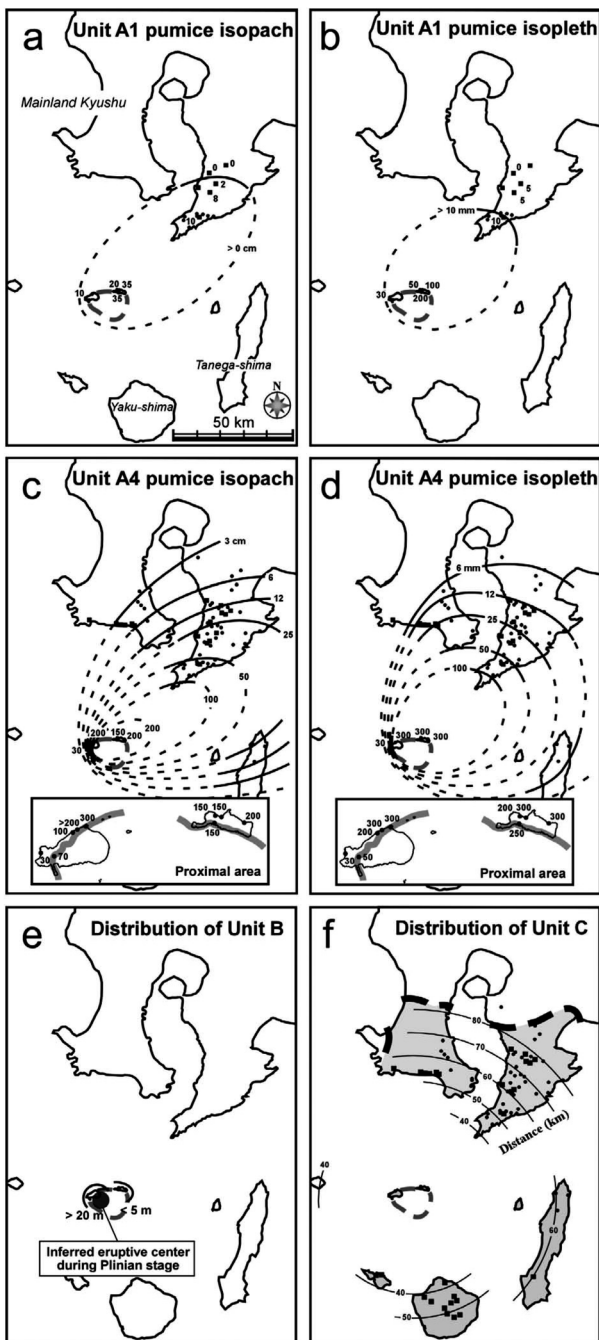


Fig. 12. (a) Isopach and (b) isopleth maps of Unit A1 pumice fall deposit, and (c) isopach and (d) isopleth maps of Unit A4 of the 7.3-ka eruption. (e) The thickness of Unit B and the inferred eruptive center during Phases 1 and 2. (f) Distribution of Unit C. Closed circles in distal area (Kyushu mainland and Tanegashima) in figures (a) and (b) and shaded area in figure (f) are based on data from Ui (1973). Closed circles in the distal area in figures (c), (d), and (f) are data from Walker *et al.* (1984). Closed circles in the proximal area and closed squares in the distal area are data from Maeno and Taniguchi (2007).

in the last 10 ky in Japan. The total estimated magma volume in the system was 70-80 km<sup>3</sup>

(DRE); the eruption therefore represents the evacuation of a major silicic magmatic system.

#### 4-1 Eruptive deposits

The eruption produced four major units, which are distributed on proximal islands (Satsuma Iwojima and Takeshima islands), on the southern Kyushu mainland, and on Kuchinoerabujima, Tanegashima, and Yakushima islands (Fig. 1). Stratigraphic sections in proximal islands are characterized by plinian pumice-fall deposits (Unit A), intraplinian pyroclastic density current deposits (Unit B), showing various types of stratification and degree of welding, and observed in only proximal islands, and climactic voluminous pyroclastic flow deposits (Units C1-C3) (Figs. 11 and 12; Maeno and Taniguchi, 2007). Units C1-C3 have been collectively named “Koya ignimbrite” by Ui (1973) in the distal area, or “Takeshima ignimbrite” by Ono *et al.* (1982) and Walker *et al.* (1984) in the proximal islands. This climactic ignimbrite is traceable up to 100 km away from the source over the East China Sea (Fig. 12), and has been interpreted as a low-aspect ratio ignimbrite by Walker *et al.* (1980; 1984) and Ui *et al.* (1984). Unit C3 can be subdivided into Units C3a, b and c. Unit C3a-b is fine-poor, lithic-rich and thickest in Satsuma Iwojima, while Unit C3c is fine-rich, pumice-rich and thickest in Takeshima (Fig. 13). The lower Unit C3a-b is thought to be co-ignimbrite lag breccia in proximal and ground layer in distal

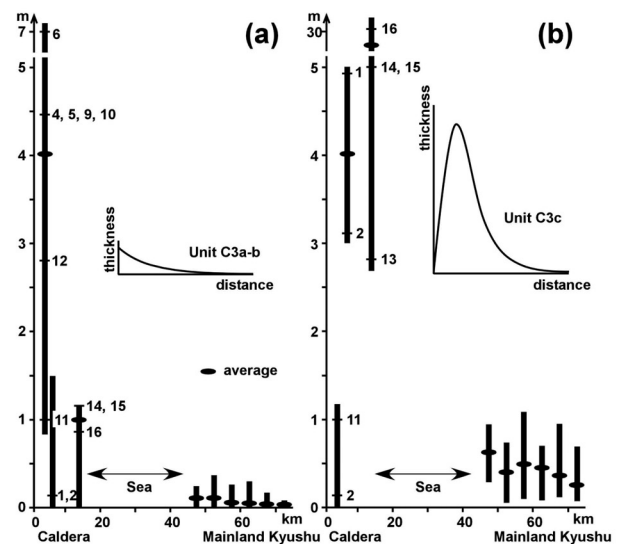


Fig. 13. Range and average values for the thickness of (a) Units C3a-b and (b) Unit C3c on proximal and distal areas. Distal data are combined with data from Walker *et al.* (1984), which are averaged for sites in 5-km distance intervals from the Kikai caldera (Maeno and Taniguchi, 2007).

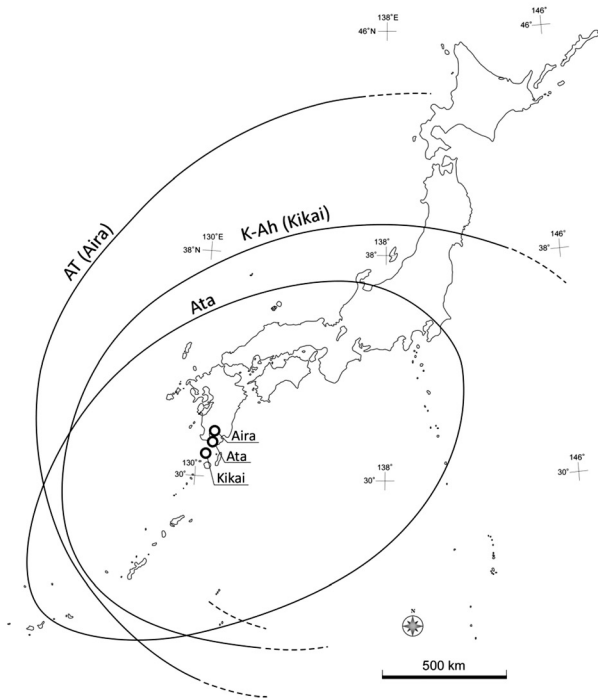


Fig. 14. Distribution of widespread ashfall erupted from the three calderas (Kikai, Ata and Aira) in southern Kyushu. Modified from Machida and Arai (2003).

areas, based on grain-size and component analyses (Maeno and Taniguchi, 2007).

The topmost Unit D is a co-ignimbrite ash-fall deposit, named “K-Ah” or “Akahoya Ash” by Machida and Arai (1978). This tephra was dispersed over a wide area of Japan, more than 1,000 km away from the Kikai caldera, and was also comparable scale to other Quaternary wide-spread tephras (AT and Ata) from southern Kyushu (Fig. 14). The sea level in this area at the time of the eruption was almost the same as at present (Ōki, 2002).

#### 4-2 Eruption sequences

A time-distance plot showing the eruptive sequences during the 7.3-ka eruption is shown in Fig.15. The plinian stage (Phase 1) is subdivided into an initial small phase and a second large one. The column height in the second phase was estimated to be 40-43 km, and the total tephra volume of this stage  $40 \text{ km}^3$  (Maeno and Taniguchi, 2007).

Collapse of the column (Phase 2) produced Unit B, which consists of multiple thin lithic-rich or pumice-rich layers or pods, including welded pumice fall layers (Maeno and Taniguchi, 2009). The deposits are characterized by stratified or cross-stratified facies and display various degrees of welding. These sedimentary characteristics indicate that during the plinian column collapse, high-temperature turbulent density currents were

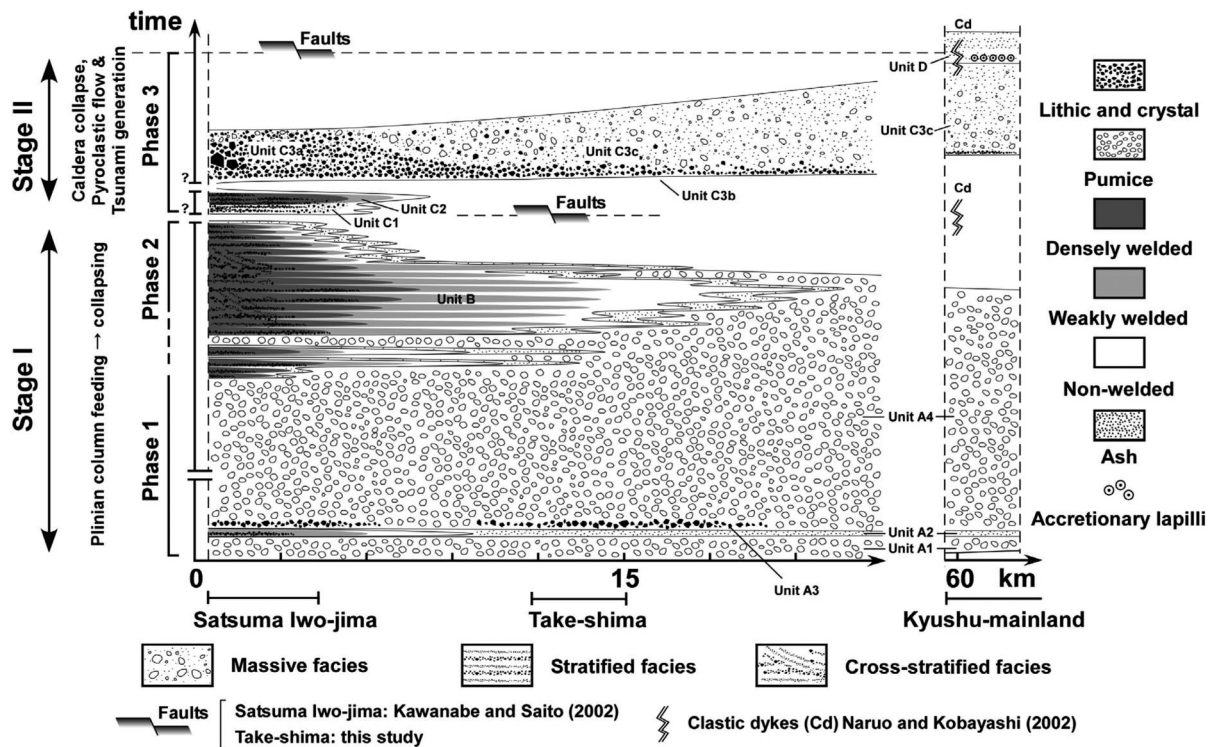


Fig. 15. Time-distance plot showing eruptive sequences and lithofacies variations of pyroclastic density currents during the 7.3-ka Kikai caldera eruption (Modified from Maeno and Taniguchi, 2007).

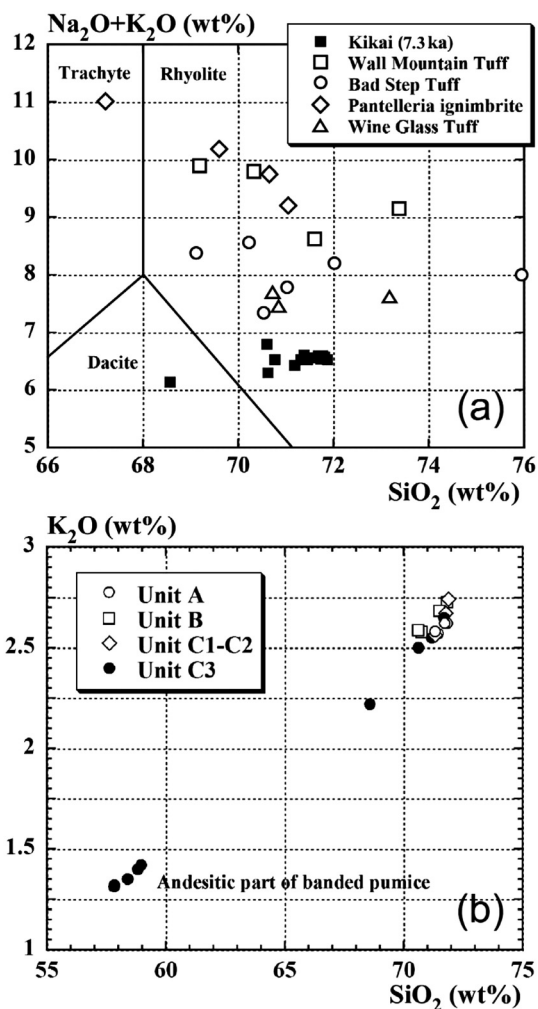


Fig. 16. Whole-rock SiO<sub>2</sub> variation diagram for (a) Na<sub>2</sub>O+K<sub>2</sub>O for silicic components (Maeno and Taniguchi, 2009) and for (b) K<sub>2</sub>O from eruptive products of 7.3-ka Kikai eruption (Maeno, unpublished data). Data from other thin or well-stratified welded tuff, similar to Unit B, are also plotted in figure (a) (Wall Mountain Tuff, Chapin and Lowell, 1979; Bad Step Tuff, Branney *et al.*, 1992; Pantelleria ignimbrite, Villari, 1974; Wine Glass Tuff, Bacon and Druitt, 1988).

generated in which the dense pyroclasts were well segregated, resulting in the lithic-rich layers or pods. Thin, well-stratified welded tuff is occasionally observed in alkali-rich products from large-scale eruptions, but the deposit of the Akahoya eruption is not significantly rich in alkali (Fig. 16a, Maeno and Taniguchi, 2009).

Phase 3 is characterized by Units C1-C3. Unit C1 shows non-welded stratified facies, which consist of lithics and crystals, including quenched juvenile materials as a minor constituent. Unit C2 displays a welded stratified facies, which consist of lithic-rich layers and pumice-rich layers. These two subunits

occur only in topographic lows on Satsuma Iwojima. Unit C3 is the thickest and is a poorly sorted non-welded massive deposit, which includes fragments of welded tuff from the underlying units on Takeshima. This indicates that multiple pyroclastic density currents produced Units C1 and C2 in the near-vent area, and were followed by the main sustained current producing Unit C3, a low-aspect ratio ignimbrite, distributed over a wide area of southern Kyushu across the sea. Co-ignimbrite ash-fall was deposited approximately contemporaneously with Unit C3. Collapse of the caldera may have started before Unit C deposition, as a fault scarp on the caldera rim is covered by Unit C in Takeshima (Fig. 15). The source appears to have been toward the western side of the caldera.

The eruption represents the evacuation of a large silicic magma chamber with estimated magma volume of 70–80 km<sup>3</sup> in DRE (Maeno and Taniguchi, 2007). The magma chamber depth of the 7.3-ka eruption is estimated at 3–7 km from the gas-saturation pressure of melt inclusions (Saito *et al.*, 2001). Banded pumices with andesitic composition in the ignimbrite (Figs. 5, 16b) indicate that mafic magma coexisted or intruded into a magma chamber deeper than approximately 7 km.

This eruption caused a huge environmental and cultural impact in the western Japan. Moreover, discovery of tsunami deposits at the east coast of the Oita Prefecture, northeast of mainland Kyushu (Fujiwara *et al.*, 2010), suggests that huge tsunamis were generated and propagated the Pacific Ocean in this eruption. Although not many geological evidences of tsunamis has been found around the caldera, numerical simulations with various initial conditions showed that a likely mechanism of tsunami generation is a rapid caldera collapse rather than entrance of a large pyroclastic flow into the sea (Maeno *et al.*, 2006; Maeno and Imamura, 2007).

## 5. Ata caldera and Ibusuki volcanic area

### 5-1 Ata eruption

The Ata ignimbrite is one of the largest Late Pleistocene ignimbrites in Japan, and erupted approximately 105–110 ka (Machida and Arai, 2003). There are two opinions on the location of the source caldera (Figs. 1, 17). Matumoto (1943) thought that the Ata caldera was located at the mouth of Kagoshima Bay (thick broken line in Fig. 17). The western caldera margin was defined by the steep scarps of the Onkadobira fault and the eastern margin by the steep western coast of the Osumi peninsula. However, Aramaki and Ui (1966),

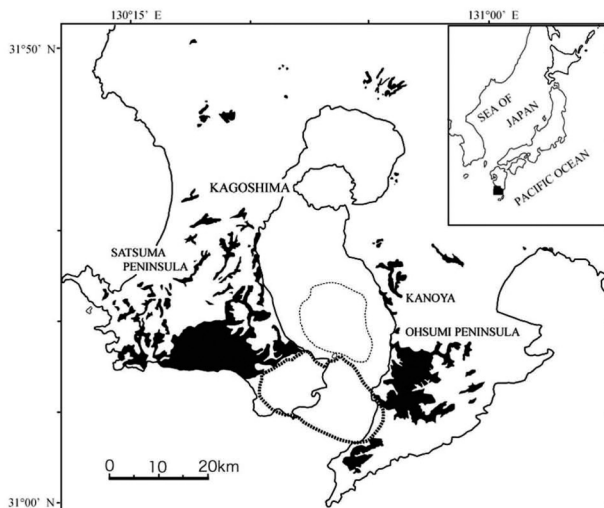


Fig. 17. Distribution of the Ata ignimbrite (Suzuki and Ui, 1982). Thick and thin broken lines show the rim of Ata caldera proposed by Matumoto (1943) and by Hayasaka (1982), respectively.

Hayasaka (1982), and Suzuki and Ui (1983) argued that the caldera depression caused by the Ata ignimbrite eruption was located to north of the caldera defined by Matumoto (1943) (shown by the thin broken line in Fig. 17). This conclusion was based on seafloor sonic prospecting data showing normal faults aligned with their revised caldera location, and the radial direction of depositional ramps outward from this source area (Fig. 18). However, post-Ata volcanism has been mainly concentrated in the Ibusuki volcanic area (Figs. 1, 19), which lies in the western portion of the Ata caldera as defined by Matumoto (1943).

The Ata ignimbrite is composed of a lower non-welded facies and an upper welded facies. The lower facies is an accumulation of thin and stratified layers; some of them are thought to be pyroclastic surge deposits. The upper welded facies is present all around the caldera and is resistant to erosion. The flat ignimbrite plateau is well preserved especially along the eastern coast of Kagoshima bay. The maximum thickness of the deposit is 100 m. The most distal deposits are more than 100 km from the center of the caldera (Watanabe, 1985).

The Ata ignimbrite has a coarse ground layer (Walker *et al.*, 1981) up to 2-m thick (Suzuki-Kamata, 1988), which is distributed mainly on the west and north sides of the caldera (Fig. 20). Suzuki-Kamata and Ui (1988) also identified an asymmetrical distribution of the welded Ata ignimbrite; this pattern was defined as “depositional ramps”. Depositional ramps can be identified in valleys wider than 1 km and decrease in scale with

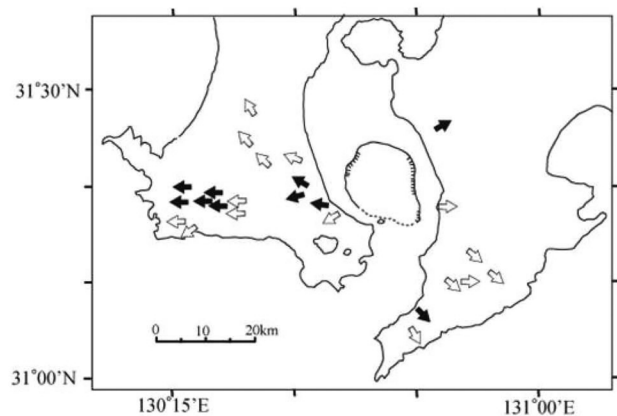


Fig. 18. Direction of depositional ramps structure of Ata ignimbrite (Suzuki-Kamata and Ui, 1988). Solid arrow: confirmed direction by field mapping and altimetry. Open arrow: estimated direction from topographic maps and aerial photograph.

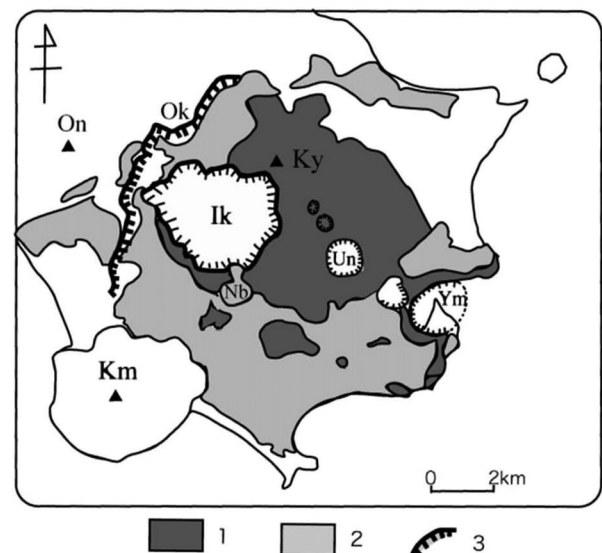


Fig. 19. Simplified geologic map of Ibusuki volcanic area (Okuno and Kobayasi, 1991, Kawanabe and Sakaguchi, 2005). Ok: Onkadobira fault scarp; On: Onodake volcano; Ky: Kiyomidake volcano; Ik: Ikeda caldera; Un: Unagiike maar; Ym: Yamakawa maar; Nb: Nabeshimadake volcano; Km: Kaimondake volcano; 1: Post Ata volcanoes; 2: Ikeda ignimbrite and related pyroclastic surge deposit; 3: Cliff including fault scarps, caldera wall, and crater rim.

increasing distance from the source. Upslope directions of depositional ramps are generally radially away from the source caldera, suggesting that the structure was formed by the flow of pyroclastic material radially away from the source (Fig. 18). The size and the gradient of the

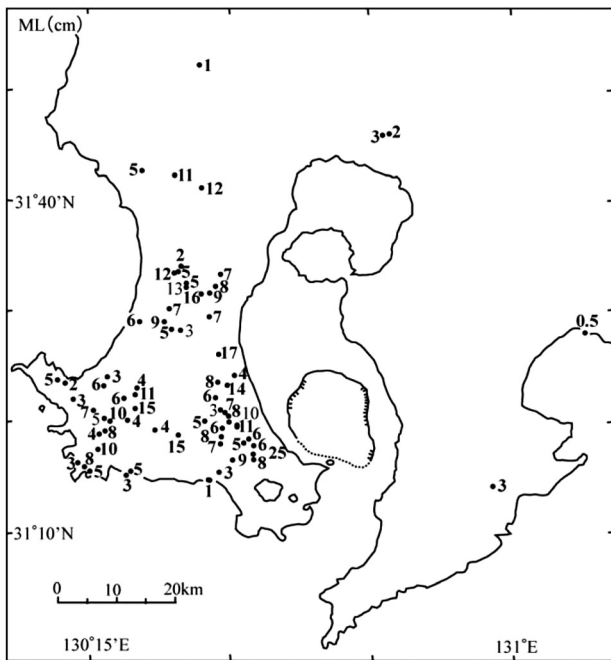


Fig. 20. Map showing the average maximum diameter of the three largest lithic clasts in an exposure of ground layer related to Ata ignimbrite (Suzuki-Kamata, 1988).

depositional ramps decrease with increasing distance from the source.

The Ibusuki volcanic area, which occupies the western half of the Ata caldera (as defined by Matumoto, 1943), is situated in the southeastern end of the Satsuma peninsula. The Onkadobira fault is part of a large system of faults that define the western margin of Kagoshima graben. Tephra from

the small Onodake stratovolcano, located on the outside of the Onkadobira fault, is overlain by Ata ignimbrite. Onodake is composed of olivine basalt, which is rare in southern Kyushu.

After the Ata eruption, many small stratovolcanoes and lava domes grew in the Ibusuki area (Fig. 21) (Kawanabe and Sakaguchi, 2005). Kiyomidake lava dome is pyroxene dacite, whose thickness is up to 200 m. Ikezoko lava is pyroxene rhyolite and the largest lava flow in this area, whose thickness is 300 m.

### 5-2 Ikeda eruption

A climactic eruption occurred at the southern flank of Kiyomidake volcano at ca. 5.7 ka and resulted in formation of the ~4 km diameter Ikeda caldera. The caldera-forming eruption was initially phreatic, later changing to magmatic. The deposits thus formed are, from the bottom to top, Ikezaki ash, Osagari scoria, Ikeda plinian pumice, and Ikeda ignimbrite (Ui, 1967; Kobayashi and Naruo, 1986). The Ikeda ignimbrite moved through topographic lows and reached the sea. The Ikeda ignimbrite has at least two flow units that have different grain-size distributions (Iwakura *et al.*, 2001).

The lower unit is relatively rich in coarse material and poor in fines smaller than 0.25 mm in diameter. The upper unit is rich in fines smaller than 0.25 mm. The upper unit has basal lithic-concentration zone (LCZ) that is observed on several localities. The lithic fragments in LCZ are derived from vent or conduit based on the rock species and emplacement temperature that was estimated by the progressive

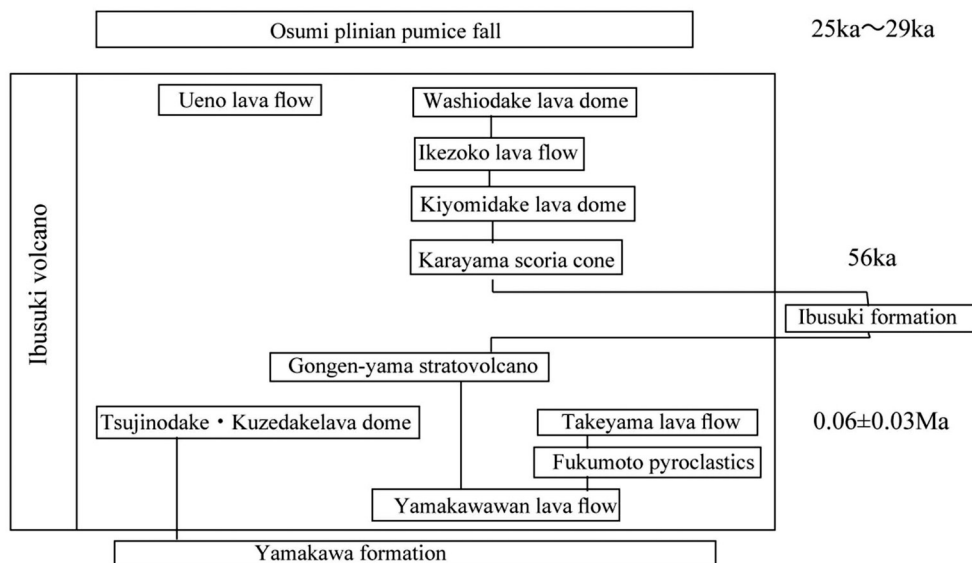


Fig. 21. Block diagram indicating the evolution of Ibusuki volcano.

thermal demagnetization method. Typical lithology at the proximal area is co-ignimbrite lag breccia. Near the caldera rim, the Ikeda ignimbrite has a proximal facies of co-ignimbrite lag breccia that consists of mainly accidental lithic fragments and pumice. It is typically clast-supported and rich in coarse lithics with a subordinate amount of pumice. The matrix is poor in fine vitric ash. Lag breccia in the west of the caldera is weakly stratified, and is composed of three lithic-enriched layers and three pumice-enriched layer alternately.

The second lithic-enriched layer corresponds to the lag breccia in the east and LCZ in the north of the caldera based on the component analysis, which suggests that the second lithic-enriched eruptive phase was the biggest phase in the Ikeda ignimbrite eruption because of the wide distribution of lithics. Many littoral vents penetrating the Ikeda ignimbrite are exposed in the coastal cliff. A littoral crater is also partially preserved at the northern margin of Kaimondake volcano. The Osagari scoria is andesite; ejecta of the following eruptions are all rhyolitic. Four maars-aligned ESE were also formed by later eruptions adjacent to the Ikeda caldera. The largest is the Yamakawa maar, which was formed by a pyroclastic surge eruption of the same rhyolitic magma.

Shortly after the caldera formation, phreatomagmatic eruptions occurred from the caldera floor, and produced the Ikedako ash, composed mainly of an accumulation of thin ash layers, with accretionary lapilli. The Ikedako ash is 10 m thick around the caldera rim. Alternations of thin layers of ash give a false impression that they are lacustrine in origin. Many clastic dikes are found in the Ikedako ash and were all penetrated from the lower horizon of the same deposit. They were probably formed by a big earthquake that occurred in the waning stage of the eruption. The total volume of magma erupted during these 5.7-ka episodes is estimated to be 5 km<sup>3</sup>.

After a long dormancy, a small lava dome, Nabeshimadake, was formed on the southeastern caldera rim at about 4.3 ka (Okuno and Kobayashi, 1991; Okuno *et al.*, 2000). As the dome grew, the northern half of the dome slid down into the caldera, due to the sector collapse of the caldera rim.

### **5-3 Eruptive activity of Kaimondake volcano**

Kaimondake volcano is undissected and consists of a basal stratovolcano and a small central volcano (Kawanabe and Sakaguchi, 2005). The first eruption occurred near the coast at ca. 4 ka, and two later eruptions were documented in 874 AD and 885 AD

(ca. 1.1 ka). The volcano was active for about 3000 years, during which 12 major eruptions occurred, named as Km-1 to Km-12 in chronological order (Fujino and Kobayashi, 1997). The mode of eruption of this volcano was mainly scoriaceous subplinian type, frequently associated with phreatomagmatic events. Lava flows were often associated with the scoria eruptions. The latest eruptions in 874 AD and 885 AD are called “Km-12a” and “Km-12b”, respectively. Among the 12 major eruption deposits, Km1 (ca. 4 ka), Km9 (ca. 2 ka), Km11 (ca. 1.5 ka), and Km12 (ca. 1.1 ka) were voluminous.

During the latest eruptions (Km12a, b), a central volcano was formed in the summit crater of the basal stratovolcano. This central volcano is not a simple lava dome, but a mound of complex volcanic materials with a composite structure. It consists of a basal scoria cone associated with fluid lava flows, later capped by a viscous lava dome.

The only subsequent activity in the Ibusuki area is that of vigorous fumaroles at several places including the Unagiike and the Yamakawa maars.

## **6. Descriptions of Stop**

The route of the field trip B6 “Kikai caldera and southern Kyushu” is indicated in Fig. 22. We spend two nights in Satsuma Iwojima, one night in Ibusuki and one night in Kagoshima city. Stops in each day are briefly introduced as below.

### **6-1 Day 1**

Meet at ferry terminal (South pier of Kagoshima harbor), and then move to Satsuma Iwojima Island by ferry boat. In the island we observe pyroclastic fallout, flow, and surge deposits of the 7.3-ka Kikai-Akahoya eruption, and stay on the island two nights (Fig. 23).

#### **Stop 1-1 Oura**

This stop is located at westernmost part of the Satsuma Iwojima (Figs. 4, 23). Well-exposed successions of 7.3-ka eruptive deposits (Unit A plinian fallout deposit, Unit B welded stratified flow deposit, Unit C non-welded/welded massive /stratified flow deposit) can be observed in a distance across a small bay (Figs. 11, 24).

We can observe also a thick rhyolite lava flow (Nagahama lava) that occurred before the 7.3-ka eruption overlain by Unit A, and basaltic and rhyolitic tephra groups from Inamura-dake and Iwo-dake volcanoes, respectively, during past five thousand years. Unit B is the densely or weakly welded stratified flow deposits. The layers mostly thin out toward higher altitudes of the caldera wall.



Fig. 22. Field trip route in all days.

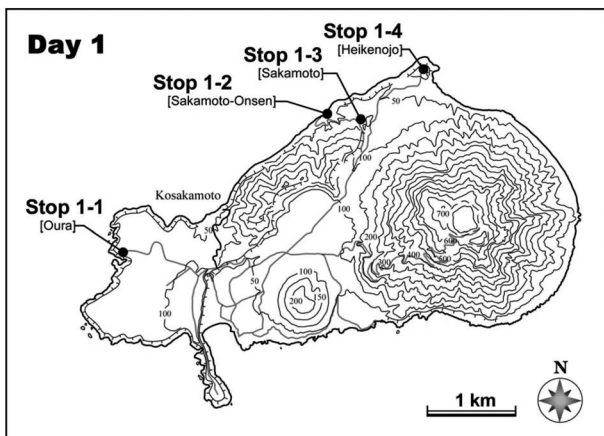


Fig. 23. Outcrop locations on Satsuma Iwojima Island in Day 1.

Unit C is composed of subunits C1-C3. Unit C1 shows non-welded stratified facies, which consist of lithic and crystals. Unit C2 displays welded stratified facies, which consist of lithic-rich layers and pumice-rich layers. These two subunits occur only in topographic lows. Unit C3 is poorly sorted, non-welded, and massive ash-pumice-rich deposit. The unit includes pumice, obsidian clasts, and other lithic fragments less than a few tens of centimeters in size.

#### Stop 1-2 Sakamoto Hot spring (Onsen)

This stop is located on the northern coast of Satsuma Iwojima (Fig. 23) and features a nice hot spring. The exposure is characterized by the upper part of the 7.3-ka deposits (Units B and C), which

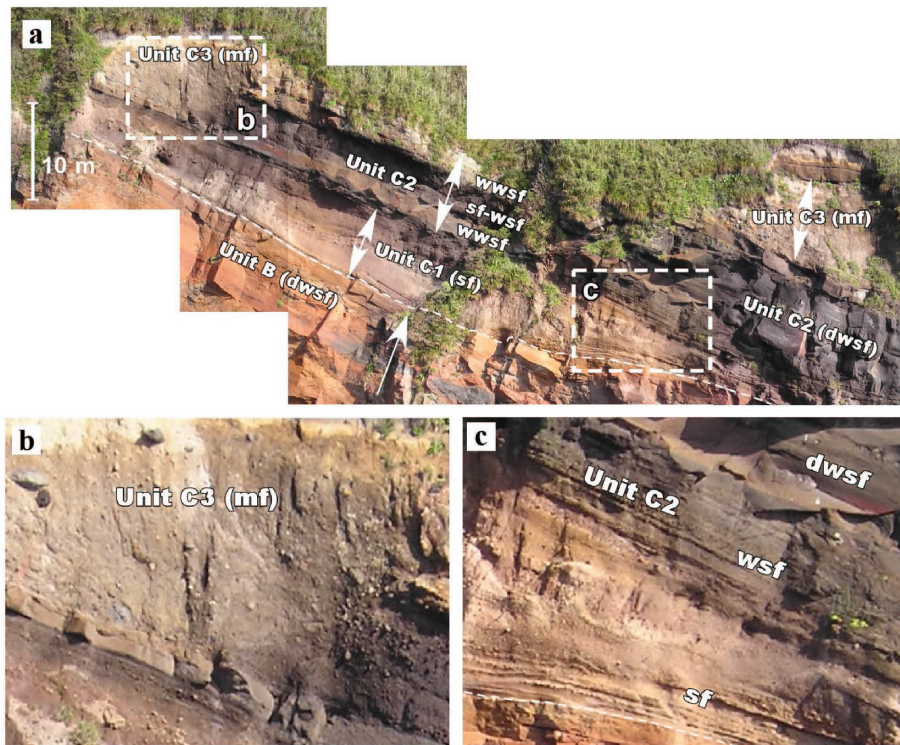


Fig. 24. (a) Unit C with various lithofacies and degrees of welding, viewed at location 1 (Oura in Satsuma Iwojima). (b) Unit C3 with non-welded massive facies and (c) Unit C2 with welded stratified facies. (Modified from Maeno and Taniguchi, 2007)

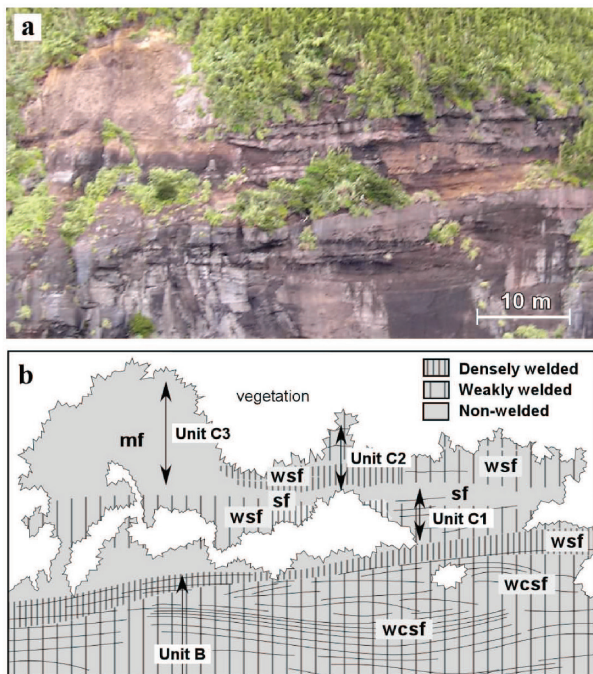


Fig. 25. (a) Photograph and (b) sketch of Units B and C with various lithofacies and degrees of welding. The lower part is Unit B with surge like cross-stratified or stratified facies. The upper part is Unit C. sf: non-welded stratified facies, wsf: welded stratified facies, wcsf: welded cross-stratified facies, mf: non-welded massive facies. (Modified from Maeno and Taniguchi, 2007)

are more than 10-m thick (Figs. 11, 25, 26). The lower part of Unit B shows stratified-to-cross-stratified lithofacies composed of thin lapilli layers. The layers occur as one or more discrete layers, lenses, or irregular-shaped pods. Centimeter-to-meter-thick layers with various degrees of welding are abundant, and often embed pumice fallout units (Fig. 26).

These lithofacies of Unit B can be observed only at Sakamoto hot spring. The major components of lithic-rich layers are altered lithic, crystals, obsidian clasts, pumice lapilli (partially welded), and glass shards. Lithic-rich pipes are sometimes vertically or horizontally developed from lithic-rich pods. The upper unit shows densely welded, stratified lithofacies, composed of welded pumice-rich layers and lithic-rich layers.

#### Stop 1-3 Sakamoto

This stop is located on northern caldera wall (Fig. 23), and we can observe top of climactic ignimbrite from the 7.3-ka eruption (Unit C3a) and basaltic and rhyolitic tephras from Inamura-dake and Iwo-dake volcanoes (Fig. 27). Ignimbrite is characterized by massive, extremely fines-poor and lithic-rich lithofacies with normal or no grading up to a few meters thick (Fig. 11). The deposits are reddish or grayish in color, reflecting a large amount

of lithic material.

**Stop 1-4 Heikenojo**

This stop is located at the northernmost point of

Satsuma Iwojima (Fig. 23). If the weather is fine, we will see Kaimon volcano on Satsuma Peninsula. The outcrop shows the 8~13 ka Komorikō tephra

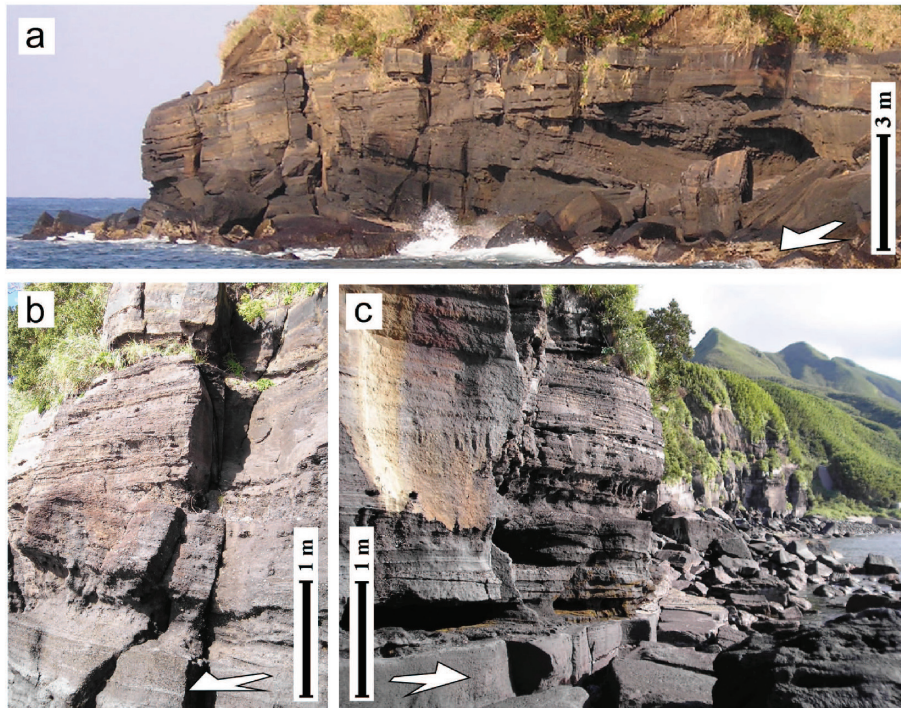


Fig. 26. (a) Surge like structures. (b) Welded cross-stratified facies and (c) stratified facies of Unit B<sub>1</sub>. Arrows indicate flow directions.



Fig. 27. Outcrop showing the eruptive history in Satsuma Iwojima after the 7.3-ka caldera-forming eruption. Takeshima ignimbrite is a product from the climactic phase of the 7.3-ka caldera-forming eruption. OIo1a~2b, In1~3, and YIo1~4a are derived from the rhyolitic Old Iwo-dake volcano, the basaltic Inamura-dake volcano, and the rhyolitic Young Iwo-dake volcano, respectively. Modified from Maeno and Taniguchi (2005).



Fig. 28. Outcrop of Heikenjo. Komorikō tephra group, 7.3-ka pumice fallout (Unit A) and ignimbrite (Unit C3), and tephra groups from Inamura-dake and Iwo-dake volcanoes. Photo was taken in 2000.

group, the plinian pumice fall of Unit A, the climactic ignimbrite of Unit C, and the tephra groups from Inamura-dake and Iwo-dake volcanoes (Figs. 11, 28). The plinian pumice fall includes large clasts, a few of which are up to ten centimeters in diameter, and is underlain by subjacent brown paleosol, which developed on top of the Komorikō tephra group. The climactic ignimbrite is characterized by a basal lithic-rich layer (Unit C3b) and overlying pumice-ash-rich layer (Unit C3c). Unit C3b is basically massive fines-poor, and includes pumice and lithics. Lithics are composed of boulder like rounded lava and altered or fresh lava. Unit C3c is massive and pumice-ash-rich. Unit B and the lower part of Unit C (Units C1 and C2) are absent, so that the upper part of Unit C (Unit C3) rests directly on Unit A. This is because of localized nondeposition or erosional removal of lower units by the upper ignimbrite.

**6-2 Day 2**

Observe eruptive products (lava flows, pyroclastic fallout, flow and surge deposits) of rhyolitic Iwo-dake and basaltic Inamura-dake volcanoes that grew up after the caldera-forming eruption. Enjoy hot spring. Stay on Satsuma Iwojima (Fig. 29).

**Stop 2-1 Nagahama North**

The upper part of the caldera wall formed by the 7.3-ka eruption is exposed at the north of Nagahama harbor (Figs. 29, 30). The outcrop represents the proximal facies of the 7.3-ka deposits: the lowermost plinian fallout deposits, densely welded intraplinian flow deposits, and the upper lithic-rich facies of the climactic ignimbrite. Deposit structures

with various degrees of welding mark the eruptive sequence in proximal during the 7.3-ka caldera-forming event.

**Stop 2-2 Higashi Hot spring**

This stop is located on the east coast between rhyolitic Iwo-dake and basaltic Inamura-dake volcano, and features a nice hot spring, Higashi-Onsen (Figs. 29, 31). We see a massive rhyolite lava flow and secondary flow deposits from the young Iwo-dake volcano (Stage YIo-II), and a basaltic lava flow (In-EL) and scoria falls from the basaltic Inamura-dake volcano.

**Stop 2-3 Erabuzaki**

This stop is located on the caldera wall at the southern end of the island. The spectacular scenery of two contrasting young volcanoes (silicic Iwo-dake and basaltic Inamura-dake) surrounded by

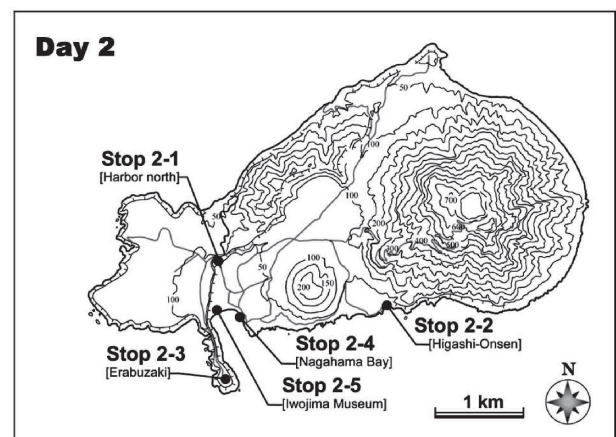


Fig. 29. Outcrop locations on Satsuma Iwojima Island in Day 2.



Fig. 30. The upper part of the caldera wall formed by the 7.3-ka eruption is exposed at the north of Nagahama harbor.

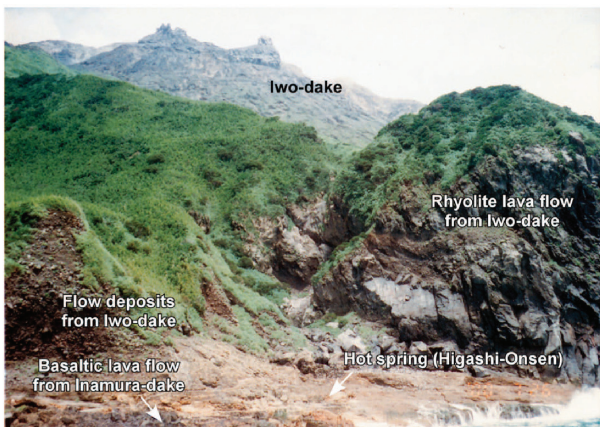


Fig. 31. Higashi-Onsen located on the east coast between rhyolitic Iwo-dake and basaltic Inamura-dake volcano, and features a nice hot spring.



Fig. 32. View from Erabuzaki on the caldera wall at the southern end of the island. The spectacular scenery of two contrasting young volcanoes (silicic Iwo-dake backward and basaltic Inamura-dake forward) surrounded by the caldera wall.

the caldera wall marks the evolution of a large silicic magmatic system beneath the sea (Fig. 32).

#### Stop 2-4 Nagahama bay

Nagahama Bay exhibits sedimentation of iron-oxyhydroxides by shallow-marine low-temperature hydrothermal activity. Its fishing port has a narrow entrance that limits exchange of seawater between the bay and open ocean, allowing the accumulation of fine-grained precipitates of iron-bearing materials (Fe-oxyhydroxides) on the seafloor (Fig. 32). The port constructed in the innermost portion of Nagahama Bay is protected from wave action by man-made breakwaters (Fig. 33). The E and W sites have different bathymetric profiles. The E site gradually slopes toward the open sea and is more than 6 m deep along the T-shape quay. The W site has a relatively flat seafloor and is shallower in the center (Fig. 33). Several small mounds (<1 m in height) occur in the central area of the E site. The W site is expected to allow the deposition of Fe-oxyhydroxides.

Preliminary sediment sampling in the fishing port recovered Fe-oxyhydroxides-rich sediments of more than 1 m in thickness. The protected nature of the fishing port would provide a unique opportunity to better understand the formation of Fe-rich sediments (Nagata, 2011; Ninomiya and Kiyokawa, 2009; Kiyokawa *et al.*, 2012).

We visit a hot spring at coast W site of the fishing

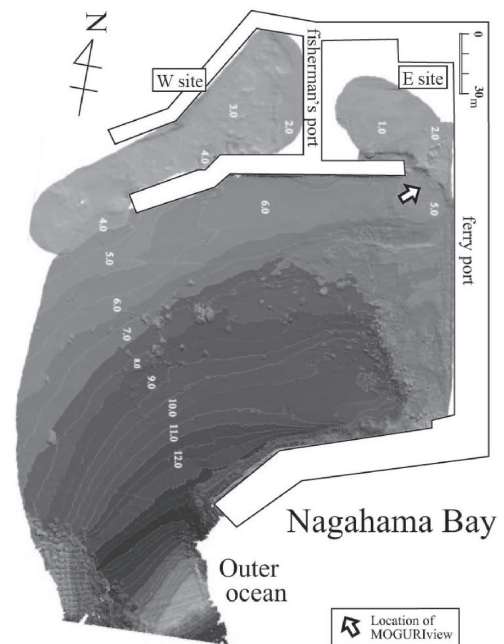


Fig. 33. Topographic map of the Nagahama bay (obtained by Mishima-mura-Kyushu University-Windy Network mapping project in 2011).

port. Hot water (pH 5.0~6.0) springs from basement brown color volcanoclastics at low tide time, and observe the simple sediment trap at W site of the fishing port. Trap starts on April 1st. See quick deposition of the Fe-oxyhydroxides. At W site, several core samples of the Fe-oxyhydroxides and reworked sediment alterations were collected (Fig. 34a, b). Ueshiba and Kiyokawa (2012) showed the thick 3 bed of tuff layers are related to heavy rain and big storm-related sediments at 2001 and 2002. During the calm condition, expected Fe-oxyhydroxides are deposited. On East side, Fe-oxyhydroxides chimney mound (bioterrace) are well preserved (Fig. 34c). It is more than 10-20 wide in area and more than 1-5 m high. It is mostly formed by very soft Fe-oxyhydroxides. Under the microscopic and SEM observation, they formed

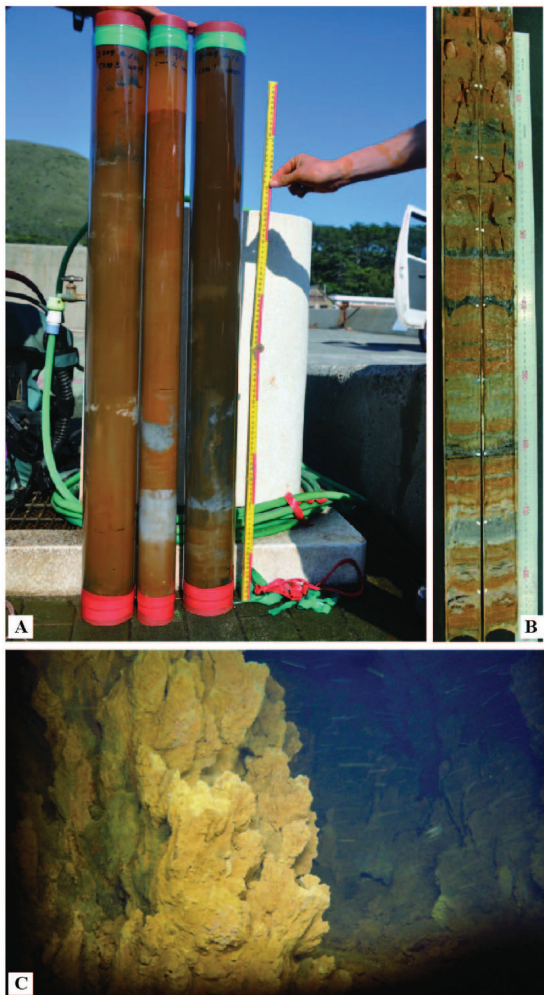


Fig. 34. A) 1-m core samples in W site. B) Half-cut samples of 1-m core from West site. Well-stratified iron-oxyhydroxides and reworked white tuff beds. C) Iron-oxyhydroxides chimney mound at E site. Photo took at 2009/April/14 10:46 AM by MOGURIview system.

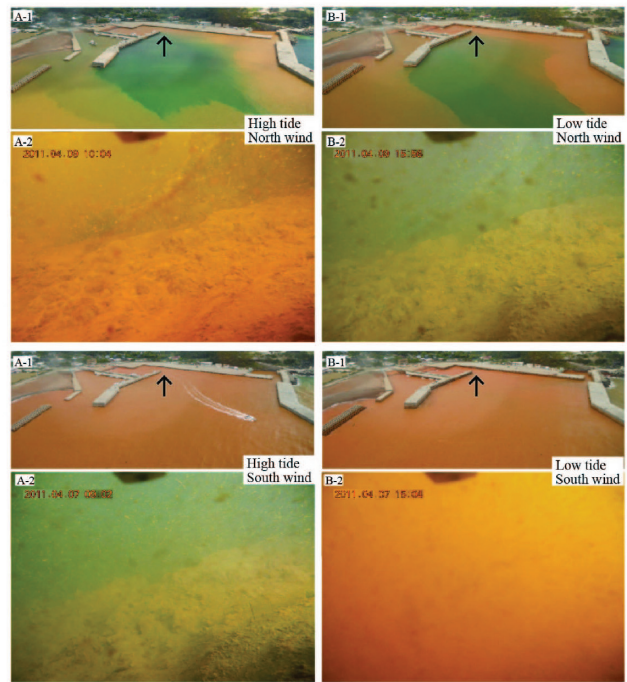


Fig. 35. Sea surface and seafloor (4.5 meter in depth) of Nagahama Bay. North wind and high tide on 9th April in 2011 (upper left). North wind and low tide on 9th April in 2011 (upper right). South wind and high tide on 7th April in 2011 (bottom left). South wind and low tide on 7th April in 2011 (bottom right). Arrow points show MOGURIview location. (Ueshiba and Kiyokawa, 2012)

twisted bacterial formed iron-oxyhydroxides. Morphologically it resembles Gallinonellaceae sp., which lived around hydrothermal systems. This mound has been forming since 1991 after dredging construction and formed T-shape fishing and ferry ports. To monitor the color of seawater in Nagahama Bay, two long-term automatic monitoring systems: MOGURIview, which observes the seawater from the seafloor, and MOGURIKU, which observes the bay from on land, were deployed (Fig. 35).

### Stop 2-5 Iwojima Science Museum

We will see several exhibitions in the museum, including “Kikai caldera diorama” and rock samples from Satsuma Iwojima. Introduction for Iwo-dake volcano and a video showing the Kikai Caldera Mapping Plan by Windy Network is also presented.

### 6-3 Day 3

Back to Kagoshima by ferry boat in the morning and then move to Ibusuki region, southeast of Satsuma Peninsula, by minibus. Observe distal facies of pyroclastic fallout and flow deposits of the 7.3-ka Kikai-Akahoya eruption, and pyroclastic deposits of explosive silicic eruptions in this area. Visit an archaeological museum exhibiting objects

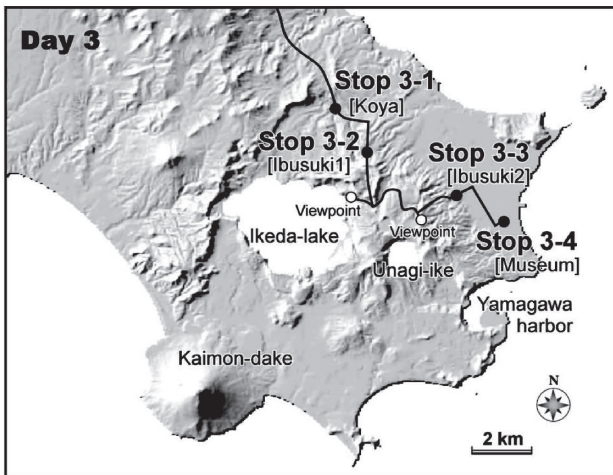


Fig. 36. Field trip route in Day 3 and outcrop locations in the Ibusuki area.

related to volcanic eruptions and their impacts in this area. Stay in Ibusuki (Fig. 36).

### Stop 3-1 Koya

We will look at the entire sequence of large-scale pyroclastic flows related to the formation of the Kikai caldera in the upper part of the exposure of

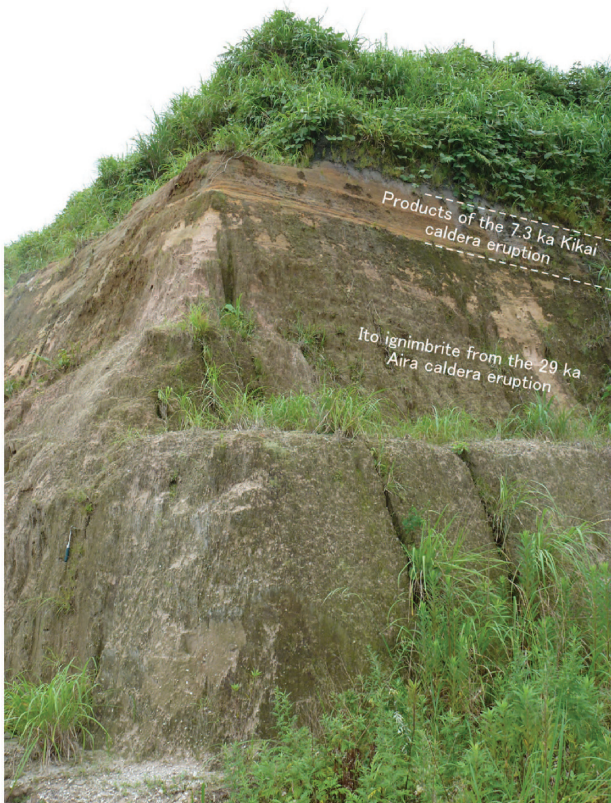


Fig. 37. The outcrop showing the deposits of caldera-forming eruptions at Aira caldera (29 ka) and Kikai caldera (7.3 ka) at Koya, near Ibusuki.

the road construction (Fig. 37). The Ito ignimbrite that formed during the Aira caldera eruption 29000 years ago is visible in the lower part of this exposure. The 7.3-ka deposit from the Kikai caldera is exposed under the upper weathered soil, consisting of plinian pumice fall deposit, Koya pyroclastic-flow deposit, and the co-ignimbrite ash fall called the “Akahoya ash”. The thickness of the 7.3-ka deposit is less than 1 m. The topmost, whitish unit is the deposit from the 6.4-ka Ikeda caldera eruption.

### Stop 3-2 Ibusuki 1

Relatively thin pyroclastic deposits from the 7.3-ka Kikai eruption and overlying ones from the 6.4-ka Ikeda eruption consist of this exposure at side of a road (Figs. 38). The lower part of this exposure is composed of older pyroclastics around the Ibusuki area. The 7.3-ka deposit from the Kikai caldera consists of plinian pumice fall deposit, Koya pyroclastic-flow deposit, and the co-ignimbrite ash fall called the “Akahoya ash”. The thickness of the deposit is less than 1 m. The upper half of this exposure consists of a series of deposits from the 6.4-ka Ikeda eruption. The deposits include Osagari scoria, Ikeda pumice fallouts, and pyroclastic surge

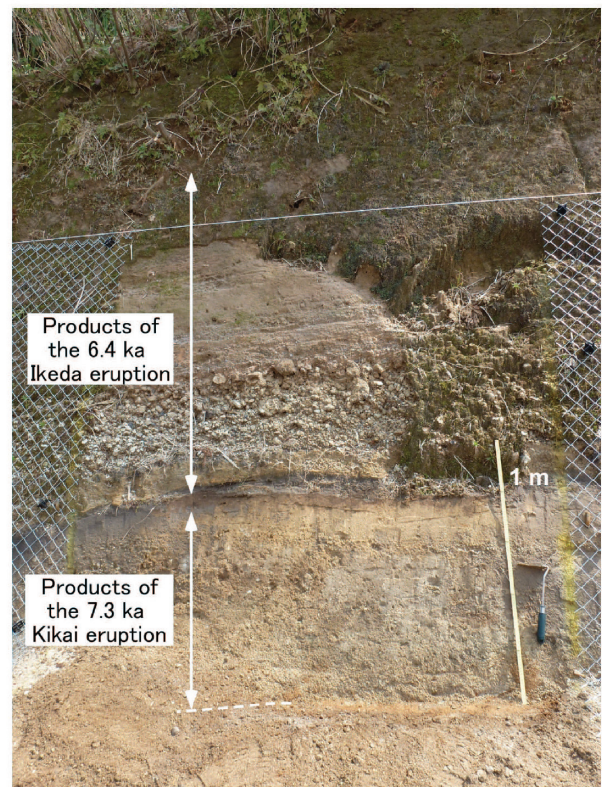


Fig. 38. The outcrop showing the deposits of caldera-forming eruptions at Kikai caldera (7.3 ka) and Ikeda caldera (6.5 ka) near Ibusuki.

deposit (Fig. 38).

**Stop 3-3 Ibusuki 2**

This outcrop is similar to Stop 3-2. We look at the sequence of plinian pumice fall, pyroclastic flows, and co-ignimbrite ash related to the formation of the Kikai caldera. The upper part of this exposure consists of a series of deposits from the 6.4-ka Ikeda eruption. The 7.3-ka deposit from the Kikai caldera consists of plinian pumice fall deposit, Koya pyroclastic-flow deposit, and the co-ignimbrite ash fall called the “Akahoya ash”. The lower part of this exposure is composed of older pyroclastics around the Ibusuki area (Fig. 39).

**Stop 3-4 Archaeological museum at Ibusuki city**

We see a lot of exhibits that mark volcanic activities and disasters caused by Kaimondake eruptions in historical times. Ash falls from the Kaimondake eruptions significantly affected human and cultural activities in this area. The museum was constructed on the archaeological site Hashimuregawa, which is also called “Japanese Pompeii”, because when deposits at the site were removed, the fields, streets, and buildings emerged



Fig. 39. The outcrop showing the deposits of caldera-forming eruptions at Kikai caldera (7.3 ka) and Ikeda caldera (6.5 ka) near Ibusuki.

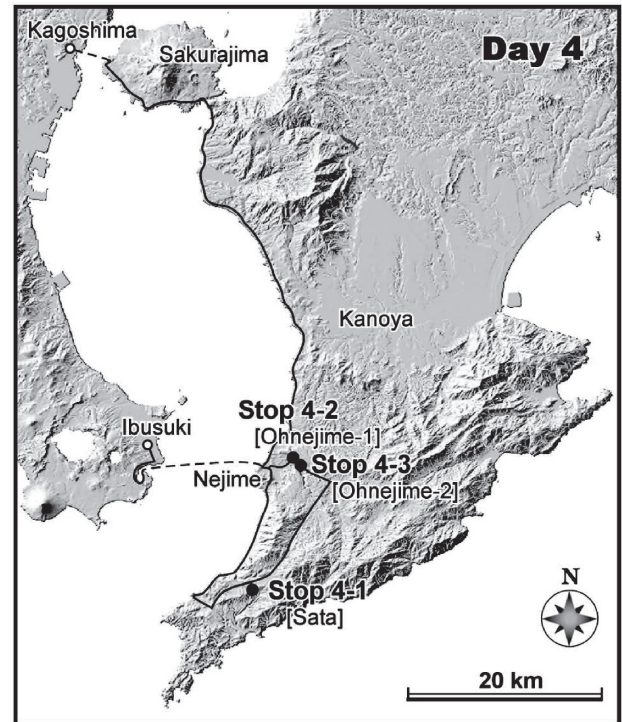


Fig. 40. Field trip route in Day 4 and outcrop locations in the Minami-Osumi region (southern part of the Osumi Peninsula).

just as they were in ancient times.

**6-4 Day 4**

Move to Minami-Osumi region, southern part of Osumi Peninsula by ferry boat and minibus. Observe pyroclastic fallout and flow deposits of the 7.3-ka Kikai-Akahoya eruption, and also welded and non-welded pyroclastic flow deposits of the Ata eruption. Move to and stay in Kagoshima city (Fig. 40).

**Stop 4-1 Sata**

Exposure of the Koya pyroclastic flow is visible on the road cut near the Sata wind power generation plant (Fig. 41). The location of the pyroclastic flow deposit 50 km from the Kikai caldera indicates that it crossed 40 km of sea and landed on Kyushu. The entire section of the 7.3-ka eruptive deposit is examined. The lowermost part is an 80-cm-thick plinian fall deposit, which is massive and contains pumice 0.5-2 cm in diameter. The ground layer underlying the Koya pyroclastic-flow deposit has a variable thickness, from 3 to 7 cm and is mostly composed of sand-sized material. The Koya pyroclastic-flow deposit is a single flow unit 80 cm thick, pumice is highly vesiculated and 4-5 cm in diameter, and segregation pipes are also observed. The top of the sequence grades into co-ignimbrite ash, which shows normal grading and contains



Fig. 41. Exposure of the 7.3-ka Kikai eruptive deposits. Plinian fall deposit, Koya pyroclastic-flow deposit, and Akahoya co-ignimbrite ash fall are observed. Segregation pipes occur in the pyroclastic-flow deposit.



Fig. 42. Exposure of the lower non-welded Ata pyroclastic-flow deposit.

abundant pumice 0.5 to 1cm in diameter.

#### Stop 4-2 Ohnejime 1

The Ata pyroclastic flow covered this region to form a pyroclastic flow plateau (Fig. 42). Columnar jointing of the welded pyroclastic flow was well exposed, but most road cuts are now covered by



Fig. 43. Exposure of the upper densely welded Ata pyroclastic-flow deposit.

cement to prevent rock-fall accidents. The lower part of the Ata pyroclastic-flow deposit is examined in this road cut. The Ata pyroclastic-flow deposit is made up of a compound cooling unit. In the lower part of the deposit thin and non-welded flow units are abundant, and these become successively slightly thicker below the welded zone.

#### Stop 4-3 Ohnejime 2

The welded part of the Ata pyroclastic-flow deposit is observed in the road cut and the lithology of densely welding processes is also commonly observed (Fig. 43). A pyroclastic flow plateau is developed only in the lower elevated proximal to medial region. In other regions, the deposit only fills the valley floor or hangs on gentle slopes underlain by the basement formation.

#### 6-5 Day 5

Depart for respective destinations.

#### Acknowledgements

We are grateful to residents of the Mishima village, Kagoshima, for their assistance during fieldwork. Special thanks go to Mr. Tatsuo Ohyama, Mr. Hideyoshi Imabeppu, Mr. Hiroshi Sato, Mr. Hisataka Sato and Mr. Goshi Hidaka for helping us during the course of our research, and also thank to H. Kamada in Board of Education, Ibusuki City, Kagoshima, for advising us useful information on outcrops in Ibusuki area. Comments from S. Yamashita and T. Ohba were helpful to improve the quality of the manuscript.

#### References

- Aramaki, S. (1984) Formation of the Aira caldera, southern Kyushu, 22,000 years ago. *J. Geophys. Res.*, **89**, 8485-8501.

- Aramaki, S. and Ui, T. (1966) Aira and Ata pyroclastic flows and related caldera depressions in southern Kyushu, Japan. *Bull. Volcanol.*, **29**, 29-48.
- Bacon, C.R. and Druitt, T.H. (1988) Compositional evolution of the zoned calcalkaline magma chamber of Mount Mazama, Crater Lake, Oregon. *Cont. Mineral. Petrol.*, **98**, 224–256.
- Branney, M.J. and Kokelaar, P. (1992) A reappraisal of ignimbrite emplacement: progressive aggradation and changes from particulate to non-particulate flow during emplacement of high-grade ignimbrite. *Bull. Volcanol.*, **54**, 504–520.
- Chapin, C.E. and Lowell, G.R. (1979) Primary and secondary flow structures in ash-flow tuffs of the Gribbles Run paleovalley, central Colorado. In *Ash-flow tuffs* (Chapin, C.E. and Elston, W.E. eds.), *Geol. Soc. Am. Sp. Pap.*, **180**, 137–154.
- Fujino, N. and Kobayashi, T. (1997) Eruptive history of Kaimondake volcano, southern Kyushu, Japan. *Bull. Volcanol. Soc. Japan*, **42**, 195-211.
- Fujiwara, O., Machida, H. and Shiochi, J. (2010) Tsunami deposit from the 7,300 cal BP Akahoya eruption preserved in the Yokoo midden, north Kyushu, West Japan. *The Quaternary Res. (Daiyonki-Kenkyu)*, **46**, 293-302. (in Japanese with English abstract)
- Hayasaka, S. (1982) Kagoshima Bay as a graben structure. In *Reports on the basement formations and subsidence structures in Kyushu* (Matsumoto, Y. ed.), Yamaguchi Univ., pp. 76-78. (in Japanese)
- Hedenquist, J.W., Aoki, I.M. and Shinohara, H. (1994) Flux of volatiles and ore-forming metals from the magmatic hydrothermal system of Satsuma Iwo-Jima volcano. *Geology*, **22**, 585–588.
- Iwakura, M., Suzuki-Kamata, K. and Kobayashi, T. (2001) Mode of emplacement of the Ikeda pyroclastic-flow deposit inferred from grain-size distribution and component data. *Bull. Volcanol. Soc. Japan*, **46**, 117-120.
- Japan Coast Guard (2008) <http://www1.kaiho.mlit.go.jp/KAIYO/kazan/kazan/kikai201015.pdf>.
- Kamada, M. (1964) Volcanic geology and geothermal features of Satsuma Iwo-Jima, Kagoshima prefecture. *Chinetsu*, **3**, 1-23. (in Japanese)
- Kawanabe, Y. and Saito, G. (2002) Volcanic activity of the Satsuma-Iwojima area during the past 6500 years. *Earth Planets Space*, **54**, 295-301.
- Kawanabe, Y. and Sakaguchi, K. (2005) *Geology of the Kaimon Dake District. Quadrangle Series, Scale 1:50,000*. Geol. Survey Japan, 82 pp. (in Japanese with English abstract)
- Kazahaya, K., Shinohara, H. and Saito, G. (2002) Degassing process of Satsuma-Iwojima volcano, Japan: Supply of volatile components from a deep magma chamber. *Earth Planets Space*, **54**, 327-335.
- Kiyokawa, S., Ninomiya, T., Nagata, T., Oguri, K., Ito, T., Ikehara, M. and Yamaguchi, K.E. (2012) Effects of tides and weather on sedimentation of iron-oxyhydroxides in a shallow-marine hydrothermal environment at Nagahama Bay, Satsuma Iwo-Jima Island, Kagoshima, southwest Japan. *Island Arc*, **21**, 66-78.
- Kobayashi, T. and Naruo, H. (1986) Phreatomagmatic deposits erupted from Ibusuki volcanic center, Japan. *Inter. Volcanol. Cong. New Zealand*, Abstract, 108.
- Kobayashi, T. and Hayakawa, Y. (1984) Geology of Kikai caldera (Source of the Koya Ignimbrite), Japan. *A progress report of the U.S.-Japan Cooperative Science Program*, 13-14.
- Kodama, K., Tashiro, H. and Takeuchi, T. (1995) Quaternary counterclockwise rotation of southern Kyushu, southwest Japan. *Geology*, **23**, 823-826.
- Machida, H. and Arai, F. (1978) Akahoya ash – a Holocene widespread tephra erupted from the Kikai Caldera, South Kyushu, Japan. *The Quaternary Res. (Daiyonki-Kienkyu)*, **17**, 143-163. (in Japanese with English abstract)
- Machida, H. and Arai, F. (2003) *Atlas of tephra in and around Japan (revised edition)*. University of Tokyo Press, 336 pp. (in Japanese)
- Machida, H., Ōta, Y., Kawana, T., Moriwaki, H. and Nagaoka, S. (2001) *Geomorphology of Japan 7 Kyushu-Nansei Islands*. University of Tokyo Press, 355 pp. (in Japanese)
- Maeno, F. and Taniguchi, H. (2005) Eruptive history of Satsuma Iwo-jima Island, Kikai, Caldera, after a 6.5 ka caldera-forming eruption. *Bull. Volcanol. Soc. Japan*, **50**, 71-85. (in Japanese with English abstract)
- Maeno, F. and Taniguchi, H. (2006) Silicic lava dome growth in the 1934-1935 Showa Iwo-jima eruption, Kikai caldera, south of Kyushu, Japan. *Bull. Volcanol.*, **68**, 673-688.
- Maeno, F. and Taniguchi, H. (2007) Spatiotemporal evolution of a marine caldera-forming eruption, generating a low-aspect ratio pyroclastic flow, 7.3 ka, Kikai caldera, Japan: implication from near-vent eruptive deposits. *J. Volcanol. Geotherm. Res.*, **167**, 212-238.

- Maeno, F., Imamura, F. and Taniguchi, H. (2006) Numerical simulation of tsunami generated by caldera collapse during the 7.3 ka Kikai eruption, Japan. *Earth Planets Space*, **58**, 1013-1024.
- Maeno, F. and Imamura, F. (2007) Numerical investigations of tsunamis generated by pyroclastic flows from the Kikai caldera, Japan. *Geophys. Res. Lett.*, **34**, L23303, doi:10.1029/2007GL031222.
- Maeno, F. and Taniguchi, H. (2009) Sedimentation and welding processes of dilute pyroclastic density currents and fallout during a large-scale silicic eruption, Kikai caldera, Japan. *Sedimentary Geology*, **220**, 227-242.
- Matumoto, T. (1943) The four gigantic caldera volcanoes of Kyusyu. *Japanese J. Geol. Geogr.*, **19**, sp., 1-57.
- Nagata, T. (2011) *Hydrothermal activity and iron sedimentation in Nagahama Bay, Satsuma Iwo-Jima Island, Kagoshima*. Master thesis, Kyushu Univ., Fukuoka, Japan. (in Japanese with English abstract)
- Naruo, H. and Kobayashi, T. (2002) Two large-earthquakes triggered by a 6.5 ka BP eruption from Kikai caldera, southern Kyushu, Japan. *The Quaternary Res. (Daiyonki-Kienkyu)*, **41**, 87-299. (in Japanese with English abstract)
- Ninomiya, T. and Kiyokawa, S. (2009) Time-series measurements of the colored volcanic vent seawaters during a tidal cycle in Nagahama Bay, Satsuma Iwo-jima Island, Kagoshima, Japan. *Mem. Fac. Sciences, Kyushu Univ., Series D, Earth and Planetary Sciences*, **32**, no. 2, 1-14.
- Nogami, K., Yoshida, M. and Ossaka, J. (1993) Chemical composition of discolored seawater around Satsuma Iwo-Jima, Kagoshima, Japan. *Bull. Volcanol. Soc. Japan*, **38**, 71-7.
- Okuno, M. and Kobayashi, T. (1991) Geology of Nabeshima-dake volcano, southern Kyushu, Japan. *Rep. Fac. Sci. Kagoshima Univ. (Earth Sci. and Biol.)*, **24**, 11-23.
- Okuno, M., Fukushima, D. and Kobayashi, T. (2000) Tephrochronology in Southern Kyushu, SW Japan: tephra layers for the past 100,000 years. *J. Soc. Human History*, **12**, 9-23.
- Ōki, K. (2002) Changes in depositional environments during the post-glacial stage in Kagoshima Bay and Seas around the Northern Part of the Ryukyu Islands. *The Quaternary Res. (Daiyonki-Kienkyu)*, **41**, 237-250. (in Japanese with English abstract)
- Ono, K., Soya, T. and Hosono, T. (1982) *Geology of the Satsuma-Io-Jima District. Quadrangle Series, Scale 1:50,000*. Geol. Survey Japan, 80 pp. (in Japanese with English abstract)
- Saito, G., Kazahaya, K., Shinohara, H., Stimac, J. and Kawanabe, Y. (2001) Variation of volatile concentration in a magma system of Satsuma-Iwojima volcano deduced from melt inclusion analyses. *J. Volcanol. Geotherm. Res.*, **108**, 11-31.
- Saito, G., Stimac, J., Kawanabe, Y. and Goff, F. (2002) Mafic inclusions in rhyolites of Satsuma-Iwojima volcano: evidence for mafic-silicic magma interaction. *Earth Planets Space*, **54**, 303-325.
- Shinohara, H., Giggenbach, W.F., Kazahaya, K. and Hedenquist, J.W. (1993) Geochemistry of volcanic gases and hot springs of Satsuma-Iwojima, Japan. *Geochem. J.*, **27**, 271-85.
- Shinohara, H., Kazahaya, K., Saito, G., Matsushima, N. and Kawanabe, Y. (2002) Degassing activity from Iwodake rhyolitic cone, Satsuma-Iwojima volcano, Japan: Formation of a new degassing vent, 1990-1999. *Earth Planets Space*, **54**, 175-185.
- Shiono, K., Mikumo, T. and Ishikawa, Y. (1980) Tectonics of the Kyushu-Ryuku Arc as evidenced from seismicity and focal mechanisms of shallow to intermediate-depth earthquakes. *J. Phys. Earth*, **28**, 17-43.
- Suzuki, K. and Ui, T. (1982) Grain orientation and depositional ramps as flow direction indicators of a large-scale pyroclastic flow deposit in Japan. *Geology*, **10**, 429-432.
- Suzuki, K. and Ui, T. (1983) Factors governing the flow lineation of a large-scale pyroclastic flow — An example in the Ata pyroclastic flow deposit, Japan. *Bull. Volcanol.*, **46**, 71-81.
- Suzuki-Kamata, K. (1988) The ground layer of Ata pyroclastic flow deposit, southwestern Japan — Evidence for capture of lithic fragments. *Bull. Volcanol.*, **50**, 119-129.
- Suzuki-Kamata, K. and Ui, T. (1988) Depositional ramps: Asymmetrical distribution structure in the Ata pyroclastic flow deposit, Japan. *Bull. Volcanol.*, **50**, 26-34.
- Tanakadate, H. (1935) Evolution of a new volcanic islet near Io-zima (Satsuma Prov.). *Proc. Imp. Acad.*, **11**, 152-154.
- Ueshiba, T. and Kiyokawa, S. (2012) Long-term observations of iron-oxyhydroxide-rich reddish-brown water in Nagahama Bay, Satsuma Iwo-Jima Island, Kagoshima, Japan. *Mem. Fac. Sciences, Kyushu Univ., Series D, Earth and*

- Planetary Sciences*, **32**, no. 4, 45-52.
- Ui, T. (1967) Geology of Ibusuki area, southern Kyushu, Japan. *J. Geol. Soc. Japan.*, **73**, 477-490.
- Ui, T. (1973) Exceptionally far-reaching, thin pyroclastic flow in Southern Kyushu, Japan. *Bull. Volcanol. Soc. Japan*, **18**, 153-168.
- Ui, T., Metsugi, H., Suzuki, K., Walker, G.P.L., McBroome, L.A. and Caress, M.E. (1984) Flow lineation of Koya low-aspect ratio ignimbrite, south Kyusyu, Japan. *A progress report of the U.S.-Japan Cooperative Science Program*, 9-12.
- Villari, L. (1974) The Island of Pantelleria. *Bull. Volcanol.*, **38**, 1-24.
- Walker, G.P.L., Heming, R.F. and Wilson, C.J.N. (1980) Low-aspect ratio ignimbrite. *Nature*, **283**, 286-287.
- Walker, G.P.L., Self, S. and Froggatt, P.C. (1981) The ground layer of the Taupo ignimbrite: A striking example of the sedimentation from a pyroclastic flow. *J. Volcanol. Geotherm. Res.*, **10**, 1-11.
- Walker, G.P.L., McBroome, L.A. and Caress, M.E. (1984) Products of the Koya eruption from the Kikai caldera, Japan. *A progress report of the U.S.-Japan Cooperative Science Program*, 4-8.
- Watanabe, K. (1985) Ata pyroclastic flow deposit in the Hitoyoshi Basin, Kumamoto Prefecture, Japan. *Mem. Fac. Education, Kumamoto Univ. Natural Science*, **34**, 55-62. (in Japanese with English abstract)